Technical Report

Manasquan River Nonpoint Source Identification Project

Monmouth County, New Jersey

Submitted to:

New Jersey Water Supply Authority
1851 Highway 31
Post Office Box 5196
Clinton, NJ 08809

Submitted by:

F. X. Browne, Inc.
P. O. Box 401
1101 South Broad Street
Lansdale, PA 19446

Table of Contents

List of Tables

List of Figures

Section 1

Acknowledgements

F.X. Browne, Inc. would like to express our gratitude to the following institutions for supporting us with this project. This report was produced with the assistance of the New Jersey DEP (NJDEP), Monmouth County Health Department (MCHD), Monmouth County GIS Management Office, South Jersey Resource Conservation and Development Council (SJRCDC), New Jersey Water Supply Authority (NJWSA), and AVOCA Engineers and Architects.

We would also like to thank Robert Schopp from the USGS and Dr. Robert Pitt, Cudworth Professor of Urban Water Systems, Department of Civil, Construction and Environmental Engineering at University of Alabama, Randy Johnson from Fondriest, Inc, Bill Richardson and Chris Heyer from YSI, Inc.

Introduction

The Manasquan River Watershed is located in Monmouth and Ocean Counties, New Jersey. The 62 square mile study area includes portions of six municipalities: Wall Township, Colts Neck Township, Howell Township, Freehold Borough, Freehold Township, and the Borough of Farmingdale. Current land use in the Upper Manasquan River subwatersheds is primarily agricultural and residential with some commercial and industrial activity.

Commercial and industrial activity is concentrated along Routes 9, 33, 34, and 35 in Monmouth County (Manasquan Watershed Management Group (MWMG), 1999). Agricultural use in the region includes a variety of crops, livestock, nurseries, sod farms, and orchards (Monmouth County, 1985, MWMG, 1999). The majority of the livestock use is horse pastures. Previous studies (e.g., Thomas, 1999) note rapid conversion of agricultural and natural lands to urban land uses in the central portion of the watershed as result of residential development.

Areas of dense population include portions of Howell Township, Freehold Township, Freehold Borough, and Wall Township (Monmouth County. 1985; NJDEPE, 1993; NJDEP, 1996). The watershed's surface drainage network includes over 140 miles of streams. Much of the stream network flows through significant riparian-floodplain-wetland complexes.

The Manasquan River is a primary drinking water supply in addition to supporting a diverse and important mosaic of freshwater and estuarine habitats. The New Jersey Water Supply Authority (NJWSA) withdraws raw water from the Manasquan River at an intake located in Wall Township, Monmouth County. Water is diverted to the nearby Manasquan Reservoir to meet the Reservoir's thirty million gallons per day (MGD) safe yield requirement (NJWSA, 2004).

The primary objective of the Manasquan River Non-Point Source Identification Project is to support NJWSA's efforts to reduce total suspended solids (TSS) and turbidity at the Wall Township intake by identifying the largest sources of land and channel derived sediment loading within the intake's 62 square mile source area watershed.

Executive Summary

The Manasquan Non-Point Source Identification Project integrates watershed modeling, existing data review, and remote sensing analysis to maximize the effectiveness of resource-intensive activities such as water quantity monitoring and stream visual assessments. F. X. Browne, Inc reviewed the following studies in formulating the project approach:

- Monmouth County Water Resources Association, March, 1999. Compilation and Assessment of Management, Regulatory and Operational Tools Available for the Manasquan River Watershed.
- Manasquan River Watershed Management Plan.1999
- T. A. Thomas, March, 1999. Manasquan River Watershed Land Development Capacity Analysis.
- MWMG, March, 1999. Manasquan River Watershed Initial Characterization and Assessment Report.
- MWMG, January, 1999. The Manasquan River Watershed: A Trend Analysis Focusing on Impacts to Water Quality.

An innovative approach to identifying sediment loading sources within the watershed was developed for use in the study. Initially, existing sources of water quality data and observations including data from the MCHD, MRWA, NJDEP and NJWSA were evaluated for trends and relationships between parameters and interaction effects. A series of remote sensing analyses including topographic, stream system, and aerial photography analysis were used to identify physical watershed conditions that may indicate elevated sediment loading from streambanks and in-stream sources.

The physical watershed factors included in the analysis were riparian buffer condition, existing land use, sinuosity, channel slope, channelization, and constrictions. A WinSLAMM model of the study area was concurrently developed. The model was parameterized and calibrated to characterize landscape derived sediment and phosphorus loading from a total of twenty-four (24) delineated subwatersheds.

The Results of the WinSLAMM modeling and remote sensing analysis were used to target stream reaches for visual assessments. Specific streambank and channel erosion problems were photographed and located with handheld GPS units. Stream visual assessments were conducted using a combination of the following protocols:

- Pfankuch, D. J., 1975. Channel Stability Rating.
- Rosgen, D. L., 1990. Bank Erodibility Hazard Rating Guide.
- Rosgen, D. L., 1993a. Stream Bank Erodibility Factors.
- U. S. Department of Agriculture, December, 1998. Stream Visual Assessment Protocol.

The visual assessment, WinSLAMM modeling, and remote sensing analyses results were used to select seven water sampling locations to more fully characterize spatial and temporal variation in sediment loading within the study area and to verify the strength of the turbidity/TSS relationship. Grab sampling was performed at the seven stream locations and analyzed for TSS, total phosphorus (TP) and turbidity. A total of eighty-four (84) samples were taken from the seven sites, seventy (70) samples were

collected during storm events and the remaining was sampled during base flow conditions. The turbidity/TSS relationship was found to be significant (R^2>0.9).

Fixed automated sampling stations were then deployed at those seven sampling locations. The fixed automated sampling stations used YSI 600-OMS multiparameter sondes that continuously monitored turbidity. The data collected from the fixed monitoring stations were evaluated at the end of a seven (7) month monitoring period and the TSS/Turbidity relationships for each sampling station was assessed.

A prioritized list of sediment source locations was compiled upon completion of the monitoring period. Results of the evaluations were used to develop sediment mitigation recommendations and reduction strategies for the prioritized locations.

Section 2 – Summary of Task 1: Assess Water Quality Data

Task 1: Assess Water Quality Data

Introduction

This section presents the results of our evaluation of existing water quality data for the 62 sq. mile Manasquan River Watershed study area. Ambient water quality data (total suspended solids (TSS), turbidity, fecal coliform and total phosphorus (TP)) from Monmouth County Health Department (MCHD), New Jersey Water Supply Authority (NJWSA) and New Jersey Department of Environmental Protection (NJDEP) were collected, standardized and organized into a Microsoft Access database. Using JMP software, linear models were developed using the resulting dataset to assess utility of turbidity monitoring as a surrogate for predicting fecal coliform, phosphorus, and TSS concentrations; to assess the range of concentrations of TSS, turbidity, TP, and fecal coliform throughout the watershed; and to describe patterns of spatial and temporal variation.

Data Management

Ambient water quality data was obtained from NJDEP, MCHD and NJWSA and combined into one dataset which was initially stored as a Microsoft Excel file. Values collected prior to 1997 were eliminated from the dataset. Records were then filtered for the following parameters: fecal coliform, TP, TSS, and turbidity. Date/time format and parameter descriptions were standardized. Latitude and longitude were standardized into decimal degrees. Non-detect values were assigned either by the listed standard deviation or as half the method detection limit. An additional field was entered to demarcate whether values were actual or were non-detects that had been replaced. Standardized data was compiled into a Microsoft Access database and information was separated into four tables (organization, parameters, sites, and water quality). This database was then linked to GIS coverage. Based on a review of methods, phosphorus data was separated into four parameter categories: TP, dissolved phosphorus, total orthophosphate, and dissolved orthophosphate. Using Access' query and pivot-table functions, TSS and Turbidity data were queried and imported into SAS Institute's JMP software to perform statistical analysis (e.g., ANOVA, multiple regressions, etc.). Data was also queried for fecal coliform and TP and imported into JMP software for similar statistical analysis.

Table 1: Sampling Site Locations and Observations by Test Parameter

		Number of Observations (N)			
Site Name/number	Site Location	Fecal Coliform	TP	TSS	Turbidity
1	Manasquan River @ Burke Rd, Freehold	38	82	0	0
1407862	Debois Creek @ Strickland Rd, Freehold	0	3	3	0
1407868	Killtime Brook @ Wyckoff Mills, Howell	0	3	0	0
6 (1407871)	Manasquan River @ Route 9 and Ford Rd, Howell	36	93	11	0
1407900	Manasquan River @ West Farms Rd, Farmingdale	0	3	3	0
1407970	Timber Swamp Brook @ Manassa Rd, Farmingdale	0	3	3	0
1407997	Marshes Bog Brook @ Yellow Brook Rd, Squankum		3	3	0
1408000	Manasquan River @ Lakewood Farmingdale Rd, Squankum	0	5	0	0
1408009	Mingamahone Brook @	0	7	0	0
1408020	Mingamahone Brook @ Route 524 Bridge	0	3	0	0
15	Yellow Brook @ Elton Adelphia Rd, Farmingdale	25	13	19	14
16-M	Squankum Brook @ Easy St, Howell	25	13	19	14
16-N	Manasquan River @ NJWSA Intake, Wall	39	82	0	0
23	Mingamahone Brook @ Belmar Blvd, Farmingdale	25	13	19	14
24	Marshes Bog Brook @ Preventorium Rd, Howell	25	13	19	14
25	Long Brook @ Howell Rd, Jerseyville	22	11	16	13
MB-2	Marshes Bog Brook @ Cranberry Rd, Farmingdale	0	3	3	0
	All Sites	235	353	118	69

*See attached Figure 6 Base Map for graphical representation of site locations.

Data Analysis

Before proceeding with the statistical analyses, we added a data field containing the season (fall, winter, spring, and summer) of sampling was added to the dataset. June 20 and December 20 were used as start dates of summer and winter respectively, and September 21 and March 21 were used as start dates of fall and spring, respectively.

An outlier analysis was performed on each parameter in JMP. Observations more than two standard deviations or greater from the overall mean were excluded from the rest of the analysis. We used a stepwise regression procedure to construct a series of linear models. In the stepwise regression, factors were considered significant at the $\alpha = 0.05$ level. In the first series of model runs, turbidity, site, and season were used to predict values of TSS, TP, and Fecal Coliform. In the second series of model runs, site and season were used as predictors of TSS, TP, and turbidity. For all model runs, interaction effects between categorical variables, site and season, were also evaluated. Standard residual pots were reviewed for trends in variance, normality, and to determine if the mean of the residuals was zero. Data was log transformed if needed to meet standard assumptions concerning the distribution of residuals. Standard ANOVA tables were generated. F tests were performed for the entire model and for individual variable effect tests.

Summary Statistics

Figures 1 through 4 below presents summary statistics for existing water quality data as a series of box and whisker and histograms. It should be noted that an outlier analysis was performed on each of the datasets below and those points considered as outliers were removed from this summarization.

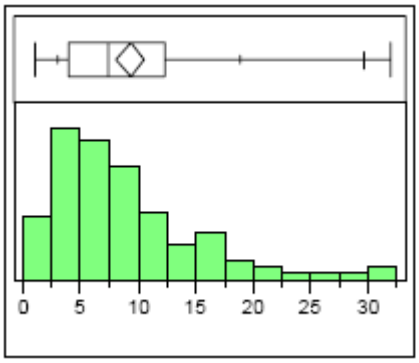

Quantiles			Moments	
100.0%	maximum	32.000	Mean	9.2886364
99.5%		32.000	Std Dev	6.9034193
97.5%		29.675	Std Err Mean	0.6008655
90.0%		18.850	upper 95% Mean	10.477292
75.0%	quartile	12.300	lower 95% Mean	8.099981
50.0%	median	7.400	N	132
25.0%	quartile	4.000		
10.0%		3.000		
2.5%		1.000		
0.5%		1.000		
0.0%	minimum	1.000		

Figure 1: Summary Statistics of TSS Data (mg/l)

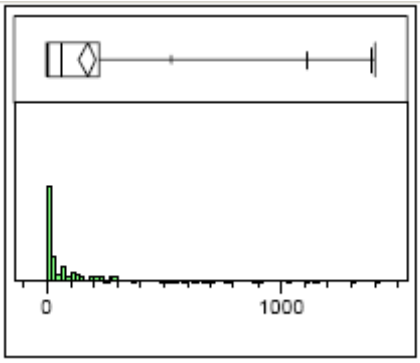

Quantiles			Moments	
100.0%	maximum	1400.0	Mean	173.20705
99.5%		1386.0	Std Dev	271.33891
97.5%		1115.0	Std Err Mean	18.009396
90.0%		532.0	upper 95% Mean	208.69486
75.0%	quartile	220.0	lower 95% Mean	137.71924
50.0%	median	60.0	N	227
25.0%	quartile	5.0		
10.0%		0.0		
2.5%		0.0		
0.5%		0.0		
0.0%	minimum	0.0		

Figure 2: Summary Statistics of Fecal Data (mg/l)

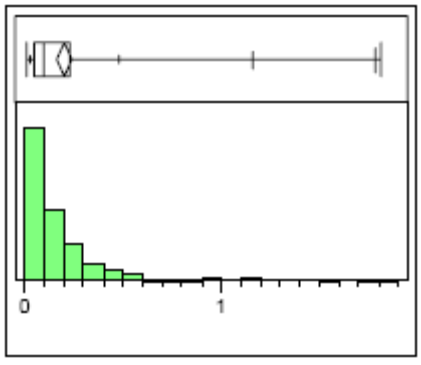

Quantiles			Moments	
100.0%	maximum	1.8100	Mean	0.2028296
99.5%		1.7841	Std Dev	0.281349
97.5%		1.1580	Std Err Mean	0.0179382
90.0%		0.4799	upper 95% Mean	0.2381623
75.0%	quartile	0.2295	lower 95% Mean	0.167497
50.0%	median	0.1005	N	246
25.0%	quartile	0.0500		
10.0%		0.0300		
2.5%		0.0109		
0.5%		0.0100		
0.0%	minimum	0.0100		

Figure 3: Summary Statistics of TP Data (mg/l)

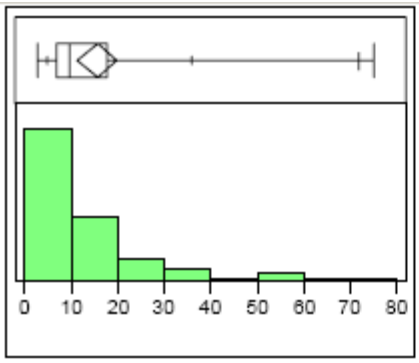

Quantiles		
100.0%	maximum	75.000
99.5%		75.000
97.5%		71.750
90.0%		36.000
75.0%	quartile	17.900
50.0%	median	9.800
25.0%	quartile	6.740
10.0%		4.680
2.5%		2.950
0.5%		2.900
0.0%	minimum	2.900

Moments	
Mean	15.587966
Std Dev	15.757742
Std Err Mean	2.0514833
upper 95% Mean	19.694456
lower 95% Mean	11.481476
N	59

Figure 4: Summary Statistics of Turbidity Data (NTU)

The tables below display the summary statistics as characterized by site location or by season. As with the box and whisker plots above, the outliers in each parameter were also removed before the summary statistics were calculated and linear regression models created. All outliers were determined by identifying points outside the 95% confidence interval and terming outlier distances using "jackknife distances," a statistical procedure that helps to identify true outliers by eliminating the influence of the outlying points on means, averages, and standard deviations (Robinson et. al., 2005).

Table 2: Summary Statistics by Site Location

	Site ID	Fecal Coliform	TP	TSS	Turbidity
		CFU/100 mL	mg/L	mg/L	NTU
	15				
Mean		*44*	*0.079*	*16.144*	*14.78*
Median		10	0.064	11.600	12.15
Min		1	0.010	4.400	4.70
Max		600	0.190	59.200	30.40
StDev		119	0.053	13.826	7.38
Observations (N)		25	13	18	14
	16-M				
Mean		*282*	*0.065*	*4.526*	*5.51*
Median		125	0.059	4.000	5.34
Min		1	0.020	1.000	2.90
Max		1210	0.120	8.000	9.62
StDev		375	0.030	1.891	1.91
Observations (N)		24	12	19	14
	23				
Mean		*142*	*0.108*	*11.979*	*15.50*
Median		65	0.060	7.800	11.08
Min		1	0.030	3.000	4.60
Max		1100	0.490	53.000	43.00
StDev		245	0.138	11.970	11.75
Observations (N)		24	13	19	12
	24				
Mean		*168*	*0.108*	*11.979*	*15.33*
Median		60	0.060	7.800	14.45
Min		1	0.030	3.000	4.90
Max		1300	0.490	53.000	32.20
StDev		288	0.138	11.970	8.21
Observations (N)		25	13	19	12
	25				
Mean		*308*	*0.168*	*16.013*	*10.15*
Median		190	0.080	7.600	7.98
Min		1	0.010	4.000	4.68
Max		1150	0.730	87.000	19.10
StDev		335	0.209	21.602	4.55
Observations (N)		21	11	15	12
	1407862				
Mean		-	*0.070*	*2.333*	-
Median		-	0.070	1.000	-
Min		-	0.060	1.000	-
Max		-	0.080	5.000	-
StDev		-	0.010	2.309	-
Observations (N)		-	3	3	-
	1407868				
Mean		-	*0.043*	-	-
Median		-	0.040	-	-
Min		-	0.040	-	-
Max		-	0.050	-	-
StDev		-	0.006	-	-
Observations (N)		-	3	-	-

Table 2: Summary Statistics by Site Location (cont.)

	Site ID	Fecal Coliform	TP	TSS	Turbidity
		CFU/100 mL	mg/L	mg/L	NTU
	1407871 or 6				
Mean		*190*	-	*6.00*	-
Median		150	-	4.00	-
Min		0	-	1.00	-
Max		770	-	16.00	-
StDev		191	-	4.84	-
Observations (N)		32	-	51	-
	1407900				
Mean		-	*0.083*	*5.000*	-
Median		-	0.090	6.000	-
Min		-	0.050	3.000	-
Max		-	0.110	6.000	-
StDev		-	0.031	1.732	-
Observations (N)		-	3	3	-
	1407970				
Mean		-	*0.150*	*3.000*	-
Median		-	0.090	3.000	-
Min		-	0.080	1.000	-
Max		-	0.280	5.000	-
StDev		-	0.113	2.000	-
Observations (N)		-	3	3	-
	1407997				
Mean		-	*0.083*	*3.333*	-
Median		-	0.100	3.000	-
Min		-	0.040	2.000	-
Max		-	0.110	5.000	-
StDev		-	0.038	1.528	-
Observations (N)		-	3	3	-
	1408000				
Mean		-	*0.036*	-	-
Median		-	0.040	-	-
Min		-	0.010	-	-
Max		-	0.050	-	-
StDev		-	0.017	-	-
Observations (N)		-	5	-	-
	1408009				
Mean		-	*0.027*	-	-
Median		-	0.030	-	-
Min		-	0.010	-	-
Max		-	0.050	-	-
StDev		-	0.015	-	-
Observations (N)		-	7	-	-
	1408020				
Mean		-	*0.073*	-	-
Median		-	0.080	-	-
Min		-	0.050	-	-
Max		-	0.090	-	-
StDev		-	0.021	-	-
Observations (N)		-	3	-	-

Table 2: Summary Statistics by Site Location (cont.)

	Site ID	Fecal Coliform	TP	TSS	Turbidity
		CFU/100 mL	mg/L	mg/L	NTU
	MB-2				
Mean		-	*0.077*	*11.000*	-
Median		-	0.090	14.000	-
Min		-	0.040	1.000	-
Max		-	0.100	18.000	-
StDev		-	0.032	8.888	-
Observations (N)		-	3	3	-
	1				
Mean		*91*	*0.353*	-	-
Median		0	0.328	-	-
Min		0	0.140	-	-
Max		2750	1.300	-	-
StDev		449	0.208	-	-
Observations (N)		38	34	-	-
	16-N				
Mean		*243*	*0.199*	-	-
Median		140	0.149	-	-
Min		0	0.070	-	-
Max		1020	1.100	-	-
StDev		260	0.177	-	-
Observations (N)		37	38	-	-

Table 3: Summary Statistics by Season

	Site ID	Fecal Coliform	TP	TSS	Turbidity
		CFU/100 mL	mg/L	mg/L	NTU
	Spring				
Mean		*256*	*0.186*	*14.24*	*12.81*
Median		140	0.121	12.00	8.05
Min		0	0.015	4.00	4.60
Max		1300	0.676	87.00	36.00
StDev		312	0.160	15.49	8.73
Observations (N)		62	44	31	18
	Summer				
Mean		*345*	*0.240*	*10.48*	*17.32*
Median		270	0.138	8.20	16.26
Min		0	0.010	2.00	4.68
Max		1210	1.700	36.80	32.20
StDev		336	0.307	9.86	11.21
Observations (N)		38	42	12	8
	Fall				
Mean		*100*	*0.153*	*6.08*	*9.20*
Median		50	0.084	5.00	9.89
Min		0	0.010	1.00	3.00
Max		530	1.300	20.00	19.10
StDev		136	0.206	4.94	4.30
Observations (N)		70	77	42	14
	Winter				
Mean		*35*	*0.159*	*12.94*	*10.20*
Median		6	0.113	8.00	9.88
Min		0	0.010	3.00	2.90
Max		800	0.548	59.20	17.08
StDev		116	0.139	13.72	4.59
Observations (N)		56	55	31	23

Linear Models

To further understand the relationship among parameters, as well as the effect of sampling station (location) and season on parameter values, we fit five linear models using a step-wise linear regression analysis in JMP.

Table 4: Regression Analyses and Statistical Models Summary

Number	Significant Predictor (X):	Response (Y):	Regression Type	Modifications	Adjusted R^2	Probability
1	Log(TURB), site, season	Log(TSS)	Stepwise	outliers excluded	0.589	<0.0001
2	site, season	Log(TSS)	Stepwise	outliers excluded	0.386	<0.0001
3	site, season, site*season[1]	Log(TURB)	Stepwise	outliers excluded	0.415	<0.0001
4	site, season	Log(FECAL)	Stepwise	outliers excluded	0.381	<0.0001
5	Site	Log(TP)	Stepwise	outliers excluded	0.332	<0.0001

[1]indicates an interaction effect

Table 5: Bivariate Regressions Predicting TSS as a Function of Season

Season	R^2	Model fit
Fall	0.196	P > 0.05
Spring	0.592	P < 0.001
Summer	0.432	P > 0.05
Winter	0.558	P < 0.0001

Table 6: Bivariate Regressions Predicting TSS as a Function of Site

Site	R^2	Model fit
Site 15	0.794	P < 0.0001
Site 16	0.028	P > 0.05
Site 23	0.030	P > 0.05
Site 24	0.191	P > 0.05
Site 25	0.165	P > 0.05

Site and Season Effects

We investigated the effect of sampling location (site) as well as sampling time (season) on concentrations of TP, turbidity, and TSS. We found significant main effects for both site and season for TSS, turbidity, and fecal coliform. We also found significant interaction effects between site and season for TSS, turbidity and fecal coliform. In the case of TP, we found only significant main effects for site with no interaction effects significant. All models were significant at the ά = 0.0001 level. However, the models were only able to explain between 33% and 59% of the total variance in the response variables.

Linear models 2-5 indicate that seasonal variation and site location have significant influences on the values of all parameters, except TP. Model No. 2 investigates the effect of site and season on TSS concentration. Model results showed that site location significantly affects TSS concentrations. Specifically, we found that sites 23, 24, 25, MB-2, & 15 had higher TSS concentrations than other sites. Stations along the main stem (1407862, 1407871, 1407900, 147970, 1407997, and 16-M) generally had lower TSS concentrations. This result may indicate dilution effects or may reflect a lack of storm flow sampling for the main stem stations. Model results also showed significant seasonal effects on TSS concentration. TSS concentrations in spring, summer, and winter were significantly different (ά = 0.05) than fall levels. Winter TSS concentrations were also significantly different than summer and spring concentrations at ά = 0.05.

Model No. 3 indicates that site location significantly effects turbidity levels (ά = 0.0001). Mean turbidity levels were lower at Site 16 than for all other stations (ά = 0.0001). Mean turbidity levels at site 25 were significantly lower than mean levels at sites 23, 24, and 15 (ά = 0.05). It is unclear why stations 23, 24, and 15 had higher levels of turbidity. Seasonally, turbidity levels are significantly lower in the summer than in any other season (ά = 0.0001). The site*season predictor represents a compound effect of the two predictors. This crossed predictor represents seasonal variation at particular sites could have significant effects on the overall fit of the model. The final model included an

interaction effect between site and season (ά = 0.001), indicating a complex relationship between spatial and temporal variation in turbidity levels. In other words, the seasonal changes at certain locations could have a significant effect on turbidity levels as a whole. These conclusions, however, are based on a limited data set and should be viewed with caution until then can be verified by further study.

Fecal coliform values are also significantly affected by site location and seasonal variations. Model No. 4 indicates that site location has a strong effect on fecal coliform concentrations. Mean fecal coliform levels at Sites 1 and 15 were significantly lower than for the rest of the sample stations (ά = 0.0001). In addition, means for sites 23 and 24 were significantly lower than sites 1407871/6, 16-N, 16-M, and 25 (ά = 0.05). Seasonally, spring and summer fecal coliform mean concentrations were higher than corresponding winter/fall means (ά = 0.0001).

Lastly, Model No. 5 indicates that TP concentration is significantly affected by site location but not season. TP concentrations at Site 1 were significantly higher than for all other sites (ά = 0.0001). TP concentrations at Sites 1407871/6, 16-N, and 1407970 were lower than for Site 1, but significantly higher than the remainder of sites. It should be noted that the method used to analyze site 1, 6 and 16-N for TP is different from the other sites and may account for some of the variance in the data. The Hach spectrophotometer method 8190 which uses an acid persulfate digestion with colorimetric measurement was used at some of the sampling events. Nearly all of the other sites utilized the ascorbic acid method as detailed in U.S. EPA method 365.1-3 and APHA method 4500-PE. The high TP concentrations recorded for Site 1 may be related to areas of agriculture in the upstream watershed. However, the high TP levels at Site 1 are somewhat peculiar considering that Site 1 also had among the lowest fecal coliform concentrations.

Turbidity Effects

We used stepwise regression to assess the utility of turbidity measurements in predicting TP, TSS, and fecal coliform. Only data collected by MCHD was used to fit the model; neither NJDEP nor NJWSA data contained turbidity measurements. NJWSA has been collecting turbidity data for the Manasquan River near the intake since 1991, although the data was not available for this analysis. We found that turbidity was not a significant predictor for fecal coliform (ά = 0.2071, R^2=0.379) or TP (ά = 0.5798, R^2=0.404). Results from an iteration showing the model with turbidity as a predictor with fecal coliform and TP is included in the appendix. In contrast, turbidity was a significant predictor of TSS (ά = 0.0001, R^2=0.589). Model No. 1 shows the best model fit for TSS when turbidity was included as a predictor. The effect of turbidity on TSS was highly significant although the percentage of variance explained by the full model was less than anticipated based on our review of several previous studies that investigated turbidity as a surrogate predictor of TSS. Inclusion of categorical variables for site location and season substantially improved model fit. The significance of the site and season terms indicates these variables modify the TSS/Turbidity relationship by shifting the y-intercept of the model. Specifically, the model showed that the TSS/turbidity relationship was significantly different for Site 16-M when compared to the other Sites. The model fit a separate intercept for spring vs. fall, winter, and summer, indicating that the TSS/turbidity relationship may also shift in the spring. Interaction effects between site and turbidity and season and turbidity were not significant indicating that the slope of the turbidity/TSS relationship remains constant regardless of site location or season. It is also important

to note that the MCHD sampling sites do not represent the upper 1/3 of the watershed. This portion of the watershed is different from the lower portion of the watershed as a result of highly glauconitic soils, steeper slopes, and more highly urban land uses. The glauconitic soils are a possible source of TSS, turbidity, and TP.

To further explore the temporal and spatial variability in the TSS/turbidity relationship, we fit bivariate regressions of TSS as a function of turbidity for each site and season. Again, outliers were removed from this analysis. Tables 5 and 6 summarize the results of these analyses. Relationships between TSS and Turbidity were markedly stronger during the spring and winter (ά = 0.001, R^2=0.592; ά = 0.0001, R^2=0.558, respectively); than in fall and summer. Relationships between TSS and Turbidity was highly significant for Site 15 (ά = 0.0001, R^2=0.794). However, bivariate regressions showed little relationship between TSS and turbidity for Sites 16, 23, 24, and 25)

Our preliminary data analysis indicates that turbidity may be used to estimate TSS levels in ambient stream water, but that the predictions of TSS may have considerable error. Our model results (R^2 = 0.589 for the full model) indicate poorer model fit than reported by other investigators. For instance, Christensen, et al. (2002) reported an R^2 value of 0.889 for TSS/turbidity Relationship for a single sampling station on the Little Arkansas River in Kansas.

The results of the bivariate regression plots indicate much stronger relationships between TSS and turbidity during winter and spring and at Site 15. Bivariate plots revealed weak, statistically non-significant relationships between the two variables during summer and fall, and for Sites 16-M, 23, 24, and 25. These results may be partially explained by the small sampling size when the dataset is separated into site and season categories; the presence of outlying leverage points that have a disproportionate influence on model fit because of the small sample size; and the relatively small range of TSS and turbidity concentrations represented at certain sites. It is interesting to note that there were no significant interaction effects between sites or season identified in the full model, indicating that the effect of site location and seasonal variation on the slopes among sites and seasons were not significantly different from one another. In other words, although the factors of site location and seasonal variation when taken individually may have an effect on the relationship of turbidity and TSS, the combination of season and site location does not appear to have any significant effect on that relationship. Instead, the model indicates that the combination of season and site on the TSS/Turbidity relationship is not significantly different from one combination to another.

Why is the model fit much “looser” than expected? We first considered the potential variance due to sampling location (different land use/slope/soil conditions), and season. We added both sampling site and season as predictors in the model to attempt to increase the model’s goodness of fit. While these terms did improve the model substantially, the overall model fit was mediocre.

We also considered the influence of flow (i.e., stage or discharge at the time of measurement), which was not explicitly measured or included as a predictor in the model. However, because of the paired nature of the data (i.e., each TSS measurement is matched with a corresponding turbidity measurement obtained at the same sampling station at the same time), we would expect the variance due to flow changes to be implicitly controlled by adding turbidity as a predictor in the model. This assumes, however, that TSS and turbidity concentrations change similarly over the course of the

hydrograph. This may be a poor assumption – turbidity (which is a measure of water clarity) and TSS (which is a measure of suspended particles) may not respond in concert to changes in flow. There are certainly temporal and spatial lags associated with storm events in terms of the relationships between these parameters. For instance, the leaching of dissolved organic material and the suspension of colloidal substances may produce a more rapid increase in turbidity on the rising limb of the hydrograph when compared with TSS. In contrast, turbidity levels may decline more slowly than TSS levels on the declining limb of the hydrograph as suspended particles are deposited, but colloidal and dissolve fractions remain in solution. Clearly, differences in response between TSS and turbidity over the hydrograph may introduce a significant source of uncontrolled variance into the TSS/turbidity relationship.

Upstream Land Use

To further understand the results of the model with respect to sampling locations, the mean values of each parameter at each sampling location were correlated to upstream land use. The results of this correlation analysis are displayed below in Figure 5. Although we did not perform effects tests, it appears that from visual inspection of the correlation graphs that there are no significant correlations between the site means of the parameters and upstream land use except for fecal coliform, which increases with increasing urban land use in the watershed.

Figure 5: Correlation of Water Quality Parameters to Upstream Land Use (% urban or % agriculture)

a.) Fecal coliform

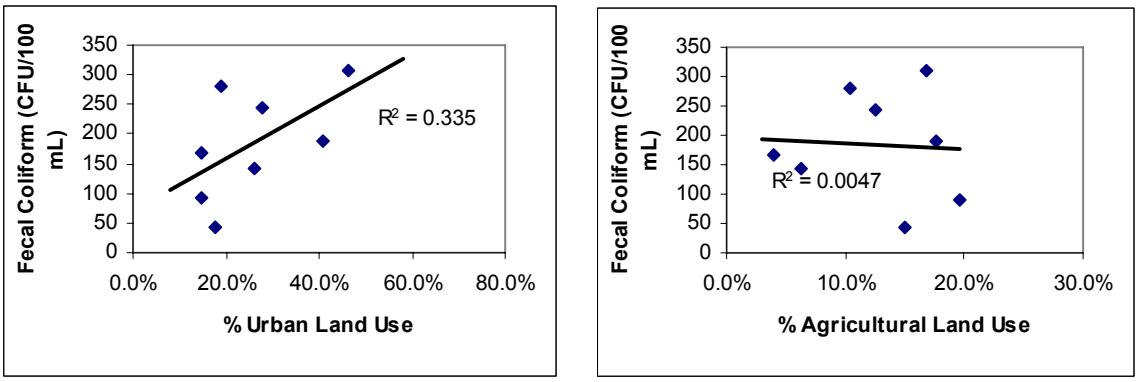

b.)Total phosphorus

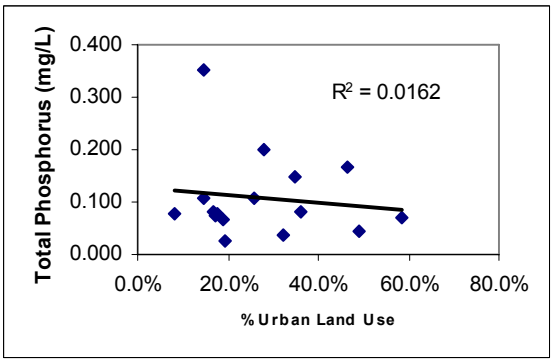

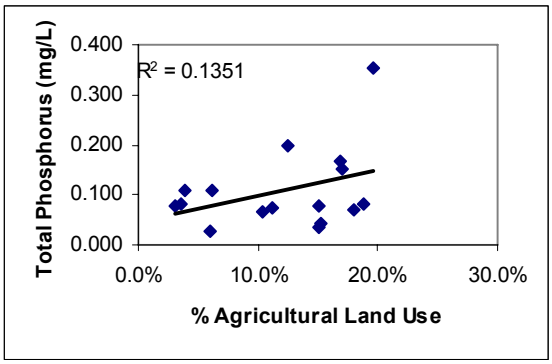

c.) Total suspended solids

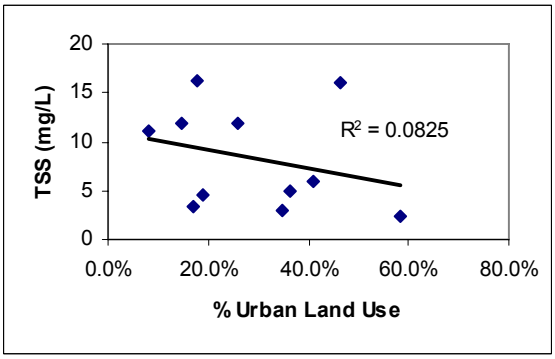

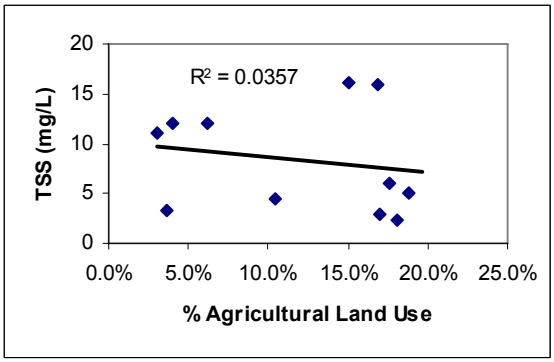

d.)Turbidity

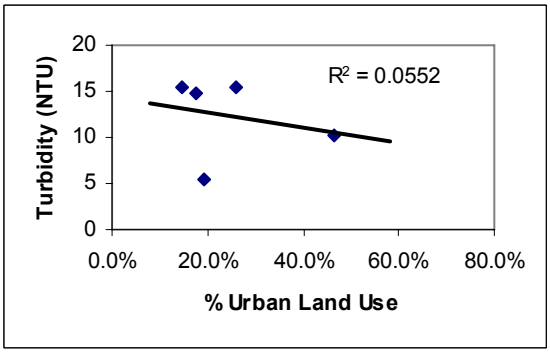

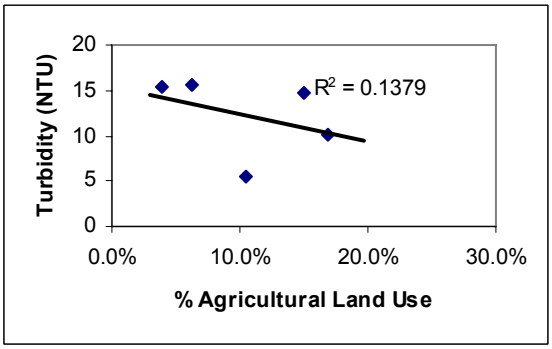

Points are station means.

Data and Analysis Limitations

The statistical models generated from the regression analysis of the compiled ambient water quality data showed certain significant relationships between predictor and response variables. It should be noted, however, that these relationships and models are based on a data set that has some significant limitations. Of particular importance is the lack of knowledge of flow conditions at the time of sampling, which is a critical factor that influences many of these variables.

Since flow conditions at the time of sampling were not reported and cannot be determined, the data set used in this analysis inevitably combines base and storm flow sampling. This effect may be somewhat minimized in Model No. 1 because each turbidity measurement was obtained at identical flow conditions (i.e., taken at the same time and place) as a corresponding TSS measurement. Thus, even though flow was not explicitly measured, the paired nature of the data would, in effect, remove the influence of flow from the data. Conversely, in the models where site and seasonal variation are the only predictors, the data is not paired and the flow conditions are unknown and unaccounted for. When comparing differences among sampling station means, it is important to note that we do not know which stations, if any, contain storm flow samples, nor what percentage of the records for a particular station were obtained during storm flow conditions. Because of our lack of knowledge about flow conditions during the time of sampling, comparisons among stations may be misleading.

Discharge Effects

Due to the limitations discussed in the initial analysis of the existing water quality data, discharge data was obtained from the USGS gauge station at Squankum and related to the existing water quality data within the database. The five linear regression models were reanalyzed to examine the effects of flow on the fit and response of the models. Results of the analysis showing all factors that were significant are presented in Table 7 and in Appendix A.

Table 7: Regression Analyses and Statistical Models with Discharge

Number	Significant Predictor (X):	Response (Y):	Regression Type	Modifications	Adjusted R^2	Probability
1	Log(TURB), site, season, discharge	Log(TSS)	Stepwise	outliers excluded	0.590	<0.0001
2	site, season, discharge	Log(TSS)	Stepwise	outliers excluded	0.395	<0.0001
3	site, season, discharge	Log(TURB)	Stepwise	outliers excluded	0.444	<0.0001
4	site, season, discharge	Log(FECAL)	Stepwise	outliers excluded	0.414	<0.0001
5	site, discharge	Log(TP)	Stepwise	outliers excluded	0.349	<0.0001

The inclusion of discharge with the analysis improved the model fit for all five of the linear regression models as shown in Table 7. All of these models had an increase in the adjusted R^2 values with $\acute{\alpha} < 0.0001$ for the overall model. Inclusion of discharge also removed the site/season interaction effect from model 3, indicating that the interactions between site and season was the result of fluctuations in the flow and not actually an effect on the turbidity values. The limited dataset however still resulted in the models fitting only 35-59% of the data.

Recommendations for monitoring

Based on our existing data analysis, we can offer several recommendations concerning the sampling approach to developing and refining TSS/turbidity relationships in the Manasquan Watershed.

1. Based on the overall model fit and level of significance, we believe that the use of automated turbidity monitoring is a useful tool for roughly predicting *in situ* TSS concentrations in the Manasquan River drainage. From our conversations with

NJWSA staff at the Manasquan Plant, heavy sediment loading is only a part of the problem; for instance, increases in color also pose operational challenges. Because turbidity measures water clarity changes due to both suspended and dissolved substances, turbidity may ultimately be a more relevant parameter than TSS given the study objectives.

2. Based on the significant site location effects, our recommendation is to stratify sampling at a number of sites throughout the watershed. Additional sites should be added to provide coverage of the upper portion of the watershed. Multiple sampling locations will allow the development of distinct relationships at each site if needed, or the aggregation of data from more than one site if site effects are not detected.
3. Based on the significant season effects, relationships developed from sampling obtained during a single season may not accurately reflect the TSS/turbidity relationship present in other seasons. Specifically, our model suggests that during spring, the TSS/turbidity relationship may be shifted when compared with fall/winter/summer relationship. Consideration should be given to expanding the grab sample collection plan to include some spring sampling.
4. Based on lack of significance of turbidity as a predictor of TP and Fecal Coliform, we recommend that TP and Fecal Coliform not be measured in the next round of grab sampling. Resources could be reallocated to expand the number of turbidity/TSS measurements. If TP and Fecal Coliform measurements are desired, we should switch to an ISCO-based sampling approach in favor of the automated turbidity approach.

Conclusions

Results of our existing water quality data review for the study area indicate that turbidity may be an adequate, if not highly accurate predicator of TSS levels in stream water within the Manasquan Watershed. Although bivariate plots revealed several weak and statistically non-significant relationships between TSS and turbidity for individual sites and seasons, based on the overall significance and fit of the full model, we would recommend proceeding with grab sampling collection to develop TSS/turbidity models for use in the project. We can reassess the utility of the turbidity-based modeling approach based on the results of the grab sampling analysis. Our results suggest that turbidity has limited utility as a predictor of fecal coliform or TP concentrations.

Our model results suggest significant spatial differences in TSS, turbidity, and TP concentration throughout the watershed, although obvious explanations for these spatial differences were, for the most part, not evident. TSS concentrations were generally higher in the tributaries draining the north central portion of the watershed in Howell Township and lower in the main stem of the Manasquan River. Many of the former areas are experiencing rapid conversion from agricultural to suburban land uses, which may help to explain the elevated levels. We found the lowest fecal coliform levels at disparate locations; Site 1, located in the headwaters of the watershed in Freehold Township and in Site 15, located in the central portion of the watershed in Howell Township. In both cases, however, the upstream watershed is largely undeveloped and as was shown in Figure 5, the trend in the study area is for watersheds dominated by urban land use to generate higher values of fecal coliform. We also found relatively low mean levels at Site 6, which is located just downstream of highly developed portions of Freehold Township and Freehold Borough. It is interesting to note that three very high results for fecal coliform were recorded at Site 6, but were removed in the outlier analysis. We found the

highest TP levels at Site 1 (which also recorded among the lowest fecal coliform levels). Other sites with elevated TP levels were located throughout the watershed without an obvious spatial pattern.

The importance of seasonal variation in fecal coliform, TSS, and turbidity levels may warrant consideration of a longer automated monitoring period in the next phase of the project.

Finally, we must stress the many limitations inherent in both the current data set and the models including lack of knowledge of flow conditions at the time of sampling, and the variability in analysis methods among datasets. The predictor values should be used with careful consideration or the data set should be expanded so the models can be fine-tuned to reflect more accurate relationships.

Figure 6: Base Map for the Manasquan River Water Supply Intake

Section 3 – Summary of Task 2: Watershed Modeling using WinSLAMM Software

Task 2: Watershed Modeling

WinSLAMM Modeling Introduction

In order to quantify sediment loading from overall land use practices within the project area, F. X. Browne Inc. conducted watershed modeling using WinSLAMM (ver. 9.0). F. X. Browne, Inc. will develop model parameters for source areas and parameter files using existing data available from MRWA, NJDEP, NJWSA, and others. In general, the level of parameterization effort will be tailored to the screening level application of the model. Aerial photography and field reconnaissance were used to verify and refine model parameters and source area delineations. Precipitation data was obtained from the South Jersey Resource Conservation and Development Council to be developed into a WinSLAMM rain parameter file. Default parameter files were used where possible in order to save time and maximize efforts. Likewise, land use classifications and watershed delineations used in the remote sensing analysis were utilized with the watershed modeling.

Methods:

Compilation of Subwatersheds

Subwatersheds to be used with the WinSLAMM model were compiled from the GIS coverage of subwatersheds created for the Remote Sensing Analysis. To ensure that the model would appropriately characterize the entire project area without excessive labor and unnecessary detail, the 364 subwatersheds from the Remote Sensing Analysis were consolidated into 24 larger subwatersheds that would encompass the major tributaries and distinctive land use areas within the project area. Areas that drained directly into the Manasquan River were delineated separately from the drainage areas of the tributaries and further divided by regional and land use differences.

Processing Howell Weather Station Rain Data

Precipitation data are required for use with the model in order to quantify the effect of storm runoff on sediment loading rates of subwatersheds within the project area. Six-minute precipitation data from the Howell weather station was obtained from the South Jersey Resource Conservation and Development Council. A total of 7.76 years of precipitation data was available from the Howell weather station and used in the WinSLAMM modeling. The precipitation data was reprocessed to fit the format necessary to be used for the WinSLAMM rain parameter file.

Updating Land Use Data

The 1997 land use/land cover GIS data was obtained from New Jersey Department of Environmental Protection (NJDEP) Office of GIS. Land use data was updated using the 2002 aerial photography coverage and 2002 urban land use coverage provided by the New Jersey Water Supply Authority. The 2002 urban land use coverage was used to identify changes between 1997 and 2002. Aerial photography was then utilized to identify those changes and the attribute tables were modified accordingly. The land use data were also verified for consistency and accuracy using the aerial photography as well as data from field reconnaissance of the watershed. This updated land use

coverage was then intersected with the subwatershed coverage to reveal the land use/land cover present in each individual subwatershed. This enabled the calculation of the overall spatial extent of the various land use/land cover types within each subwatershed and identified dense urban areas from rural agricultural areas.

Delineating Typical Source Areas

The WinSLAMM model requires the characterization of source areas to quantify source loading within watersheds and subwatersheds. This process can be very time and labor intensive, if one were to characterize source areas of every detail in a subwatershed, especially those of the size in this study. Instead, a procedure of selecting representative samples of land use/land cover types and characterizing the source areas within that smaller, more manageable sample space was employed. Using the aerial photography from 2002, source areas such as rooftops, driveways, parking lots, landscape areas, playgrounds and roadways were delineated and their areas calculated within ArcGIS. The percentages of each of these source areas as a part of the land use/land cover type were calculated. At least three samples of each land use/land cover type within the entire project area were used to delineate the source areas. Their values were averaged, and the resulting average was used to calculate the percentages of each source area type per land use/land cover type.

Incorporating Soils

Soil conditions and soil porosity have a great effect on runoff and infiltration. WinSLAMM takes this into consideration and requires that source areas be defined also according to the hydrologic soil groups underlying each source areas. Since, WinSLAMM only considers two soil types sandy soils in hydrologic soil groups A and B and silty soils in hydrologic soil groups C and D, soil data obtained from the Natural Resource Conservation Service (NRCS) was first defined as sandy or silty according to these hydrologic groups. Land use/land cover data that had been intersected with the subwatersheds were then intersected with this modified soil data to create land use/land cover types that were defined by subwatershed and soil type.

Calculating Subwatershed Source Areas

With source areas delineated and defined according to soil type and land use/land cover type and subwatershed areas calculated, the calculations of source areas within each subwatershed could be performed. Using a Microsoft Excel worksheet, the source area percentages were applied to the land use/land cover data that had been defined by subwatershed and soil type. This results in a table of each subwatershed being partitioned into land use types defined by WinSLAMM, the corresponding soil type underlying it, and the source areas within that partition. This is the data that is needed to parameterize the WinSLAMM model to the Manasquan project area.

One final step was to define this dataset according to estimates of areas connected to the stormwater discharge system. Applying the estimated connectivity percentages for each source area using the percentages listed in the report on the Delaware and Raritan Canal Tributary Assessment and Nonpoint Source Management Project Watershed Restoration and Protection Plan reproduced in Table 8 below, the data was finalized and ready for input into the WinSLAMM model.

Table 8: Percent Land Use "Connected" to Stormwater System (estimated)

WinSLAMM land use	NJDEP land use	Roof	Driveway	Paved Parking	Unpaved Parking	Playground
Residential	Rural Residential	0	50	50	50	0
	Low Density Residential	25	100	100	50	0
	Medium Density Residential	50	100	100	50	0
	High Density Residential	100	100	100	50	0
Commercial	Commercial	100	100	100	50	0
Industrial	Industrial	100	100	100	50	0
Freeway	Transportation	100	100	100	50	0
Institutional	Recreational	100	100	100	50	0
Other urban/ Open Space	Forest Shrub/Brush Wetlands Water	0	50	50	50	0
	Agriculture	0	50	50	50	0

From Delaware and Raritan Canal Tributary Assessment and Nonpoint Source Management Project Watershed Restoration and Protection Plan (NJWSA, 2006)

Results:

Table 9: Source Area Percentages and Land Use Classifications

Land Use	WinSLAMM Land Use	Roof %	Driveway %	Road %	Paved Parking %	Small Landscape %	Large Landscape %	Unpaved Parking %	Playground %	Undeveloped %
Rural Residential (RUR)	Residential	8	2	10	1	78	0	1	0	0
Low Density Residential (LDR)	Residential	12	4	11	1	71	0	0	1	0
Medium Density Residential (MDR)	Residential	18	2	25	2	52	0	1	0	0
High Density Residential (HDR)	Residential	35	5	14	5	40	0	0	1	0
Commercial/Services (COM)	Commercial	30	7	20	35	8	0	0	0	0
Industrial (IND)	Industrial	40	5	15	30	10	0	0	0	0
Athletic Fields / Recreational (REC)	Institutional	0	5	10	5	0	65	5	10	0
Schools/Institutional (SCH)	Institutional	30	7	15	35	5	5	0	3	0
Transportation (TRAN)	Freeway	0	0	95	0	5	0	0	0	0
Military Reservations (MIL)	Institutional	30	10	25	25	5	0	0	0	5
Transitional/Built-up Land (TSL)	Freeway	0	0	5	0	0	0	85	0	10
Forest (FOR)	Open Space	0	0	10	0	0	0	0	0	90
Water (WTR)	Open Space	0	0	0	0	0	0	0	0	100
Wetlands (WET)	Open Space	0	0	10	0	0	0	0	0	90
Cropland/Pastureland (CROP)	Open Space	7	1	8	0	3	0	1	0	80
Nurseries/Other Agriculture (AGR)	Open Space	7	2	10	1	20	25	5	0	30

Table 9 above summarizes the source area characterizations by both the NJDEP land use classifications and the equivalent land use classifications used in the WinSLAMM modeling. The source areas were characterized in GIS using land use data obtained from Monmouth County GIS Office and adjusted with 2002 urban land use data. They were then adjusted to reflect land use changes as shown in the 2002 aerial photographs. One day of field reconnaissance was used to verify the accuracy of the land use classifications. The source area percentages are the average of source area percentage calculations from three samples of each NJDEP land use classification.

Table 10: Subwatershed Area Breakdown by WinSLAMM Land Use Classification

SUBSHED ID	RESIDENTIAL (Acres)	COMMERCIAL (Acres)	INDUSTRIAL (Acres)	FREEWAY (Acres)	INSTITUTIONAL (Acres)	OPEN SPACE (Acres)	TOTAL (Acres)
1	253.15	15.50	0.12	14.23	0.00	2117.35	2400.35
2	882.10	90.00	0.00	44.21	0.00	282.02	1298.33
3	6.47	0.00	0.00	1.82	0.00	410.29	418.58
4	544.16	47.86	0.00	5.79	17.36	276.00	891.17
5	437.01	200.18	23.05	83.27	17.21	333.11	1093.84
6	1511.43	359.34	312.06	156.59	16.31	1247.80	3603.52
7	1883.88	400.33	347.13	213.51	18.00	2243.21	5106.07
8	225.84	9.62	0.00	3.28	0.00	561.25	799.99
9	467.70	43.06	38.80	18.92	3.45	582.30	1154.23
10	186.77	40.33	18.31	84.55	10.49	716.15	1056.58
11	140.69	36.98	15.20	37.73	4.33	527.74	762.65
12	243.27	39.34	61.01	1.60	9.69	1708.89	2063.80
13	396.70	15.02	0.00	172.19	12.80	2122.73	2719.43
14	85.65	9.78	30.55	0.00	42.82	1397.64	1566.44
15	208.90	39.61	126.38	0.94	57.97	2268.66	2702.45
16	42.80	0.00	0.00	28.48	9.34	844.99	925.61
17	266.04	27.65	15.91	40.98	337.10	2821.87	3509.57
18	691.58	110.37	142.68	215.36	307.10	6117.05	7584.14
19	220.69	36.69	27.88	29.99	0.00	1806.86	2122.11
20	227.14	13.84	0.00	9.76	0.00	463.21	713.94
21	906.98	64.90	10.13	25.52	7.25	1642.59	2657.38
22	280.89	8.91	16.81	18.20	13.59	1042.03	1380.43
23	70.77	12.00	14.48	67.80	23.77	563.39	752.21
24	38.60	18.05	2.19	51.79	0.00	1704.66	1815.30
Grand Total	10219.19	1639.37	1202.69	1326.52	908.58	33801.79	49098.12

Table 10 above summarizes the land use areas within each sub-watershed using the classifications used in the WinSLAMM model. For spatial reference of the sub-watershed locations, refer to the attached GIS map entitled, Map of Watersheds Used in WinSLAMM. Using the data included in these two tables and incorporating soils data, source areas were calculated for each individual sub-watershed. This is the data that is actually entered into WinSLAMM to proceed with the source loading models. Each sub-watershed was processed as an individual WinSLAMM run and the results of the WinSLAMM modeling are presented in Table 11 below.

Table 11: Summary of WinSLAMM Results

Subshed ID	Subshed Area (acres)	Total Runoff Volume (ft3)	TSS (pounds)	TSS (Tons)	TSS per year (Tons/yr)*	TSS per unit area (tons/ac)	TP (pounds)	TP (Tons)	TP per year (Tons/yr)*	TP per unit area (tons/ac)
1	2400.35	527900000	27730000	13865	1787	5.78	16992	8.50	1.09	0.0035
2	1265.95	344000000	7798000	3899	502	3.08	23350	11.68	1.50	0.0092
3	524.53	294200000	14210000	7105	916	13.55	17729	8.86	1.14	0.0169
4	937.87	288400000	5143000	2572	331	2.74	11248	5.62	0.72	0.0060
5	1059.98	945900000	12630000	6315	814	5.96	12188	6.09	0.79	0.0057
6	3505.55	1756000000	29110000	14555	1876	4.15	39874	19.94	2.57	0.0057
7	4988.69	1866000000	36130000	18065	2328	3.62	50953	25.48	3.28	0.0051
8	948.94	159800000	4730000	2365	305	2.49	8277	4.14	0.53	0.0044
9	1563.50	301600000	7166000	3583	462	2.29	14073	7.04	0.91	0.0045
10	1052.52	262500000	6917000	3459	446	3.29	7885	3.94	0.51	0.0037
11	776.65	180600000	4602000	2301	297	2.96	6464	3.23	0.42	0.0042
12	2059.88	472500000	12030000	6015	775	2.92	15379	7.69	0.99	0.0037
13	2594.59	390100000	9203000	4602	593	1.77	13183	6.59	0.85	0.0025
14	1898.80	385500000	11370000	5685	733	2.99	12970	6.49	0.84	0.0034
15	2720.56	692000000	19350000	9675	1247	3.56	22072	11.04	1.42	0.0041
16	910.66	230400000	7279000	3640	469	4.00	7756	3.88	0.50	0.0043
17	3427.32	945900000	24030000	12015	1548	3.51	25296	12.65	1.63	0.0037
18	7412.61	2188000000	56210000	28105	3622	3.79	59755	29.88	3.85	0.0040
19	2190.62	497100000	13710000	6855	883	3.13	15916	7.96	1.03	0.0036
20	705.80	189600000	4416000	2208	285	3.13	7685	3.84	0.50	0.0054
21	2660.82	799300000	30130000	15065	1941	5.66	30358	15.18	1.96	0.0057
22	1332.75	290200000	7189000	3595	463	2.70	10375	5.19	0.67	0.0039
23	737.28	197100000	4838000	2419	312	3.28	4963	2.48	0.32	0.0034
24	1715.80	388400000	11560000	5780	745	3.37	11753	5.88	0.76	0.0034

*Based on 7.76 years of real-time precipitation data from Howell Weather Station

The results of the WinSLAMM model runs for the 24 subwatersheds that were delineated from the Manasquan study area are presented in Table 11. These results are based on the parameterization steps outlined in the methods and using the precipitation data obtained from the South Jersey Resource Conservation and Development Council. The subwatersheds are shown on the map entitled: *Figure 7: Map of Subwatersheds used in WinSLAMM.*

A cursory analysis of the results shows that subwatersheds 6, 7, 17, 18 and 21 produced the most TSS within the study area. Subwatersheds 6 and 7 are transitional areas from the urban center of Freehold borough to a predominantly agricultural land use area. Subwatershed 21 is the region within the study area that is seeing markedly increased development of subdivisions and new residential areas. Subwatershed 17 is dominated by the military institution which contains large surface areas of imperviousness. Subwatershed 18 is another mixed use area where natural and agricultural lands transition into the urban center of Farmingdale. Subwatershed 18 also contains a portion of the regional airfield near Farmingdale. However when TSS yield is normalized to a per unit area calculation, it is noticed that subwatersheds 3, 5, and 21 produce the most sediment per area. Subwatershed 3 is dominated by a quarry and this may explain the high rate of sediment production. Subwatershed 5 is at the heart of Freehold borough, but in an area of glauconitic soil known to be highly erosive and possible source for TSS, turbidity, and TP.

Taking a cursory look at the TP results, subwatersheds 6, 7, 17, 18 and 21 again produce the highest yields of total phosphorous. However, subwatershed 15 is not far off from the lowest value in that group. These results show that among these transitional watersheds, the areas where agricultural land use dominates such as in subwatersheds of 7 and 18, TP yield are generally higher. This can also be seen by the generally higher TP values for the whole northern mid-section of the study area (subwatersheds 7, 9, 11, 12, 15, and 18).

Figure 7: Subwatersheds used in WinSLAMM

Figure 8: Annual Total Phosphorus Loads from WinSLAMM Modeling

Figure 9: Annual Total Phosphorus Yields from WinSLAMM Modeling

Figure 10: Annual Total Suspended Solids Loads from WinSLAMM Modeling

Figure 11: Annual Total Suspended Solids Yields from WinSLAMM Modeling

Section 4 – Summary of Task 2: Watershed Modeling using Remote Sensing

Task 2: Watershed Modeling

Remote Sensing Modeling Introduction:

In order to quantify sediment loading from channel processes such as streambank erosion and streambed incision, F. X. Browne Inc. employed remote sensing analyses to assess the over 140 miles of stream channel contained within the study area. Through remote sensing analysis, "at-risk" stream segments were selected for detailed field characterization via visual assessment. The analysis involved quantifying five risk factors to infer channel sediment loading characteristics for channel segments throughout the watershed.

1. Streams surrounded by highly altered riparian land use are less stable due to the removal of root systems that protect stream banks from erosion in less disturbed corridors.
2. Near bank soils with high erodibility are more prone to the weathering effects of stream flow. Over time, streambanks with highly erodible soils are more likely to exhibit rapid lateral rates of erosion and transmit higher sediment loads.
3. Streams with high channel slopes are generally more susceptible to channel change (e.g., stream incision) as well as bank mass wasting and failure.
4. Rapid upstream land use changes (particularly conversion from agricultural or natural lands to urban uses) lead to increased channel-derived sediment loads as increases in impervious surfaces increase peak discharges and the frequency of bankfull (channel forming) flow events.
5. The intensity of urban land uses tend to correlate with widening, incised, unstable channels that generate significant quantities of sediment

Methods

We used GIS and remote sensing analysis to delineate stream segments and to determine subindex values and total index scores for each stream segment. Subindex values for each of the five factors listed above were assigned to ranges in their values. The ranges were identified at natural statistical breaks in each of the respective datasets so that each of the subindex values are distributed evenly across the whole dataset and reflect the overall range of parameter values.

Stream Segment Delineation

The hydrography of the study area, obtained from Monmouth County GIS, was divided into stream segments initially by tributary junctions. Segments greater than 3,000 feet long were further divided into more manageable segments at points of riparian land use change as observed in 2002 aerial photography of the study area. Using the soil survey GIS coverage, segments that still exceeded 3,000 feet in length were further divided at soil polygon intersections. Using aerial photography, the stream segments were aligned and segments that were identified as features that were not streams such as irrigation ditches or cranberry bogs were removed from the stream coverage. Individual stream segments were then assigned a unique "segment ID" number. This process resulted in a total of 391 stream segments with lengths ranging from 300 to about 2500 feet and averaging 1775 feet in length.

Riparian Land Use

Using the stream segment GIS coverage, riparian land use was analyzed. A 15 foot buffer was created for the stream segment coverage and the land cover GIS coverage from 1997 was clipped to the buffer. Riparian land use was assessed for percentage of stream length adjoined by non-natural land cover. Natural land cover consists of wetlands, wooded and other natural, unaltered areas. Non-natural cover therefore would consist of all the urban, agricultural and other land cover types that have altered the land. These values were then assigned an index value from 0-10, with 10 representing a stream segment adjoined entirely by non-natural land cover within the 15 foot buffer area.

Table 12: Sub index Values for Riparian Land Use as Percent Stream Length Adjoined by Non-natural Cover

Sub index	Range	
0	0.000	1.070
1	1.070	4.770
2	4.770	8.690
3	8.690	12.980
4	12.980	18.880
5	18.880	26.350
6	26.350	34.490
7	34.490	45.830
8	45.830	60.170
9	60.170	78.560
10	78.560	99.890

Near-Bank Soil Erodibility

To quantify erodible soils within the riparian corridor, water erodibility K factors were attained from the Natural Resource Conservation Service (NRCS) for each soil unit. Soils with higher K factors are more erodible according to previous studies performed by the NRCS and others (NRCS, 2005, Wischmeier and Smith, 1978). K factors for each soil unit were entered and the soil coverage was clipped to the stream segment buffer. For each stream segment, the average soil erodibility within the 15 foot buffer region was calculated and entered into the dataset. Again, stream segments were each assigned a subindex value from 0-10 based on the average erodibility K-factors of each segment, with 10 representing segments flowing through the most erodible soils.

Table 13: Sub Index Vales for Soil Erodibility K Factors

Sub index	Range	
0	0.000	0.090
1	0.090	0.218
2	0.218	0.320
3	0.320	0.400
4	0.400	0.473
5	0.473	0.560
6	0.560	0.665
7	0.665	0.770
8	0.770	0.997
9	0.997	1.300
10	1.300	2.100

Channel Slope

Channel slope was calculated for each segment using USGS topographic maps and a spot elevation coverage provided by the Monmouth County GIS. Stream slopes were calculated from the 2 foot contour surface generated from the spot elevation coverage. Each stream segment was assigned a third sub index value from 0-10 based on channel slope, with 10 representing segments with the steepest slopes.

Table 14: Sub Index Values for Channel Slope (ft/ft)

Sub index	Range	
0	0.000	0.022
1	0.022	0.043
2	0.043	0.064
3	0.064	0.085
4	0.085	0.107
5	0.107	0.129
6	0.129	0.151
7	0.151	0.171
8	0.171	0.193
9	0.193	0.215
10	0.215	0.237

Upstream Land Use Change

The last factor assessed in this remote sensing analysis of the study area was land use change. GIS coverages for land use/land cover were obtained from New Jersey Department of Environmental Protection (NJDEP) Office of GIS.

In order to assess the study area for these land use/land cover changes, we first delineated drainage areas for each individual segment. Each drainage area needed to incorporate the upstream flow as well. We manually delineated an upstream drainage

area for each of the 391 stream segments using USGS topographic maps and 2-foot contours created from spot elevation data provided by Monmouth County GIS. Once these drainage areas were delineated, the percent imperviousness was calculated for each watershed and land cover type.

Table 15: Sub Index Vales for Upstream Impervious (%)

Sub index	Range	
0	0.00	2.00
1	2.00	4.45
2	4.45	7.78
3	7.78	11.10
4	11.10	14.30
5	14.30	19.10
6	19.10	25.20
7	25.20	32.30
8	32.30	38.80
9	38.80	46.80
10	46.80	54.30

To determine the change in land use between in 1986 and 1997, the land use/land cover data layer from 1986 was intersected with land use/land cover data from 1997, which was published on November 1, 1998. The resulting intersection coverage was used to identify polygons where land use/land cover had changed between 1986 and 1997. This new land use/land cover data layer was then intersected with the stream segment drainage area coverage to identifying areas where land use/land cover had changed within each individual drainage area. Intersection polygon areas were recalculated. We then determined the change in impervious cover from 1986 to 1997 for each intersected polygon. These values were then summed by drainage area to yield the change in impervious cover on an absolute and percentage basis for each drainage area. Values for impervious cover change were normalized to a 0 to 10 scale.

Table 16: Sub Index Values for Upstream Change in Impervious Cover (acres)

Sub index	Range	
0	-17.550	-12.660
1	-12.660	-2.880
2	-2.880	3.420
3	3.420	9.840
4	9.840	21.300
5	21.300	38.690
6	38.690	77.340
7	77.340	145.020
8	145.020	247.700
9	247.700	486.210
10	486.210	705.180

We were not able to obtain land use/land cover data more recent than 1997. However, NJWSA provided updated urban land use polygon coverage for 2002. Using this

coverage, we determined the change in percent urban land use for each drainage area between 1997 and 2002. Percent impervious was calculated using aerial photography and the land use/land cover data; areas of impervious cover was divided by total area each drainage basin to attain percent impervious values. Values for impervious cover change could not be calculated because the 2002 data contained only polygons representing urban land use. Thus, we used the percentage increase in urban land use as the predictor variable rather than change in impervious cover.

Table 17: Sub Index Values for Change in Upstream Urban Land Use (%)

Sub index	Range	
0	-0.404	-0.253
1	-0.253	0.004
2	0.004	0.015
3	0.015	0.035
4	0.035	0.057
5	0.057	0.105
6	0.105	0.178
7	0.178	0.313
8	0.313	1.004
9	1.004	7.330
10	7.330	20.351

Determination of Index Values

In order to formulate a ranking system to identify "at-risk" stream segments, the subindex values for each factor summed to yield a final index score. Each subindex score was weighted equally in the final index value. Subindex values for channel slope, near bank riparian land use, and near bank soil erodibility were calculated as described above.

In considering the final land use change index values, we wanted to incorporate the concept that the effect of a unit increase in imperviousness varies according to the existing level of imperviousness in the watershed. Specifically, the literature suggests that unit increases in percent imperviousness influence stream health most profoundly when existing imperviousness is moderate (Cappiela and Brown, 2001, Brant and Kauffman, 2000, Arnold and Gibbons, 1996, and Center for Watershed Protection, 2003). By contrast, at very high or low values of existing imperviousness, the influence of increase in percent imperviousness is minimal. To account for this effect, we modified both the 1986-1997 impervious change index value and the 1997 -2002 urban land use change subindex value as described below.

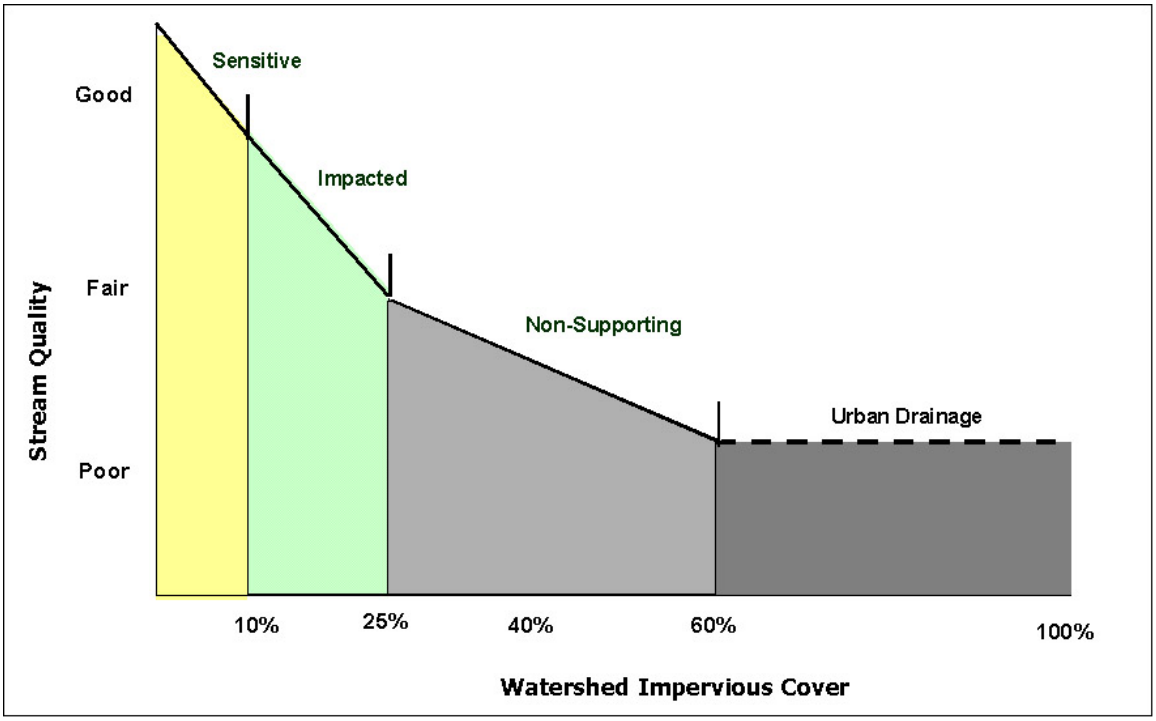

Figure 12: Illustration of Impervious Cover and its Impact on Stream Quality (Center for Watershed Protection, 2003)

Adapting the standard Gaussian growth curve (Spiegel, 1992) and fitting it to relationships identified for imperviousness and stream health (i.e., points of inflections in impervious vs. stream health curve and point of maximum stream health decline as shown in Figure 1), a mathematical model (see Equation 1 below) was extrapolated to identify the relationship between imperviousness and the significance of land use and land cover change. This model shows that in a drainage area that is either relatively natural (% impervious <10) or is already highly developed (% impervious > 30), the significance of incremental land use or land cover change is minimal, but in those areas where imperviousness indicates rapid change in land use and land cover (% impervious approximately between 15% and 20%), unit land use changes become very significant (Brant and Kauffman, 2000; Brun and Band, 2000). Equation 1 was used to adjust subindex values for the land use/land cover change from 1986-1997 and the % urban land use change from 1997-2002 to reflect the relationships discussed above.

$$F' = F \cdot e^{-0.25 \cdot (5 - \%IMP)^2} \qquad \text{(Equation 1)}$$

Where:

F' = adjusted subindex value for land use/land cover change in drainage area
F = initial subindex value for land use/land cover change in drainage area
%IMP = subindex value for % Impervious in drainage area

The exponential portion of the equation above generates a bell-shaped curve with the highest value being equal to the number one (1). This peak occurs when the %IMP subindex score has a value of 5 which correlates to when percent imperviousness ranges from 14% to 19%. Land use/cover changes with %IMP subindex scores of 5 will therefore not be changed. On the other hand, %IMP subindex scores either less or

greater than 5 will generate a value for the exponential portion of equation 1 progressively less than one depending how great a difference.

$$I = F_1^{'} + F_2^{'} + F_3 + F_4 + F_5 + F_6 \qquad \text{(Equation 2)}$$

Where:

I	=	overall index score
F_1'	=	adjusted subindex value for land use/land cover change from 1986-1997
F_2'	=	adjusted subindex value for % urban land use change from 1997-2002
F_3	=	subindex value for % impervious in drainage area
F_4	=	subindex value for near bank soil erodibility
F_5	=	subindex value for near bank land use
F_6	=	subindex value for channel slope

Using Equation 2, we calculated an overall index value for each stream segment. Without adjusting F_1 and F_2, Equation 2 would yield index scores ranging between 0 and 60. Since F_1 and F_2 were adjusted to reflect relationships concerning unit increases in imperviousness, their adjusted subindex scores may be lower than their initial values. Observed overall index scores ranged from 0 to 42, with 42 being the most critically "at-risk" stream.

Results:

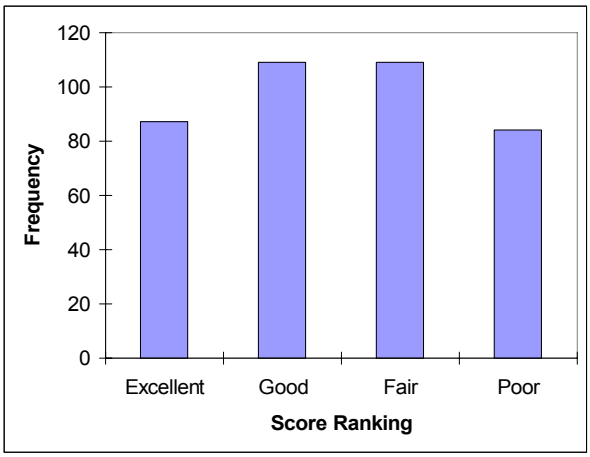

Figure 13: Histogram of index scores from remote sensing analysis

As shown in Figure 2 above, the remote sensing analysis shows that approximately half of the stream segments in the study area have index values that indicate that they are in good or excellent condition with respect to sediment loading risk. There are a total of 84 segments that are classified as poor and are severely "at risk" for channel sediment loading. These score rankings can also be viewed spatially in the attached Stream Ranking Map as well; stream segments with a poor index rank are marked in red and segments ranked excellent are shown in green.

Selection of Visual Assessment Reaches

As mentioned in the introduction, the goal of the remote sensing analysis is to identify the most probable locations of sediment loading from channel processes such as stream bank erosion and streambed incision and to rank stream segments with respect to the risk of sediment loading from those channel processes. We decided to field verify the remote sensing analysis by visually assessing a sub-set of the fair and poor-rated stream segments. In order to select representative visual assessment segments, we first needed to divide the fair- and poor-ranked segments into homogenous groups. To do this, we used a recursive partitioning method using SAS Institute's JMP statistical software. The portioning process recursively splits the dataset into groups based on a series of factor (X) variables such that variance in a single response (Y) variable around the group means is minimized and the variance of the group means around the overall mean is maximized. In this case, we selected the subindex score variables as the factor variables and the total index score as the single response variable. Through this partitioning process, the fair and poor-rated segments were divided into eight groups.

Using the results of the partitioning process, two to three representative segments were selected from each group for detailed visual assessment. To best represent each partition, one segment was selected from the center of the group, where segments were close to the mean score of the group, while the other segment(s) were selected from both high and/or low scoring segments. Using this process, a total of twenty segments were selected for detailed visual assessments. Segments already assessed by the Manasquan River Watershed Association were excluded.

Reference Reach Selection

A reference reach was selected from among the unimpaired segments as determined by the score ranking of remote sensing analysis. The reference reach, defined as a stream segment that has the best attainable channel condition given the prevailing physiographic setting, provides a benchmark against which the level of impairment as recorded in the visual assessments can be compared. We selected the three segments with the lowest total rankings (Segments 228, 263, and 264) as potential reference reach segments. After reviewing the three potential reference reach segments, we found segment 228 to have the lowest score; however it was situated in an inaccessible area and could not be selected. Of the remaining two segments which both had the same score, we chose segment 264 as our reference reach for its accessibility and condition.

Figure 14: Stream Ranking Map from Remote Sensing Analysis

Section 5 – Summary of Task 3: Visual Assessments

Task 3: Visual Assessments

Visual assessments of the Manasquan River Watershed were performed by the staff of F. X. Browne Inc., between November 29, 2005 and December 29, 2005. A total of twenty-one segments were assessed, including one reference reach, as discussed in the previous section of Remote Sensing. The purpose of the visual assessment process was to identify stream segments within the Manasquan River Watershed that are geomorphically unstable and are likely sediment sources to downstream areas. A windshield survey had also been conducted earlier on November 16, 2005 by a member of the F. X. Browne Inc. staff together with staff members from the New Jersey Water Supply Authority and the Manasquan River Water Treatment Facility who had firsthand knowledge of the problem areas within the watershed. Figure 17 shows the locations of the stream segments/sites that were visited on the windshield survey. Several of the stream segments ranked as good and excellent in the remote sensing analysis were visited during the windshield survey. Field notes and photographs are included in the appendix.

The following field methods were used to rank the stream segments:

1. The Vermont Rapid Geomorphic Assessment for Unconfined Streams
2. The Pfankuch Channel Stability Rating
3. The Rosgen Bank Erodibility Hazard Index

Each stream segment was assessed according to the three methods listed above and given a score for each method. These scores were then added together giving each stream segment an overall total. Overall scores ranged from worst (0), to best (10.01). Of the twenty-one segments assessed, stream segment number 18 ranked the worst, with an overall score of 0, and segment number 193 ranked the best with an overall score of 9.93. Segment number 264, the reference reach, had the highest score of 10.01.

The main types of degradation seen on the Manasquan River included incision, widening, and aggradation. Some planform changes were seen as well. Incision was indicated by deepened stream channels with eroded, vertical banks; nick points and head cuts in the channel and its tributaries; and steepened sediment bar faces. Widening indications included erosion on both sides of the stream along a large portion of the segment; undermined banks with exposed roots, unstable trees and vegetation; debris in the channel; slumping or mass failures of the banks into the stream; as well as fine sediments in the stream channel bottom, with mid and side-channel bars present. Possible aggradation was occurring as well, evidenced by fine sediments observed in the stream channel bottom. Planform changes were noted, but were not as prevalent as incision, widening, and aggradation. Flood chutes and channel avulsions, change in bed form structure, oddly placed scour pools, and island formation were indications of changes to the planform. The most dramatic examples of degradation were seen along the main stem of the Manasquan, on segments 15, 17, 18, and 30. The least degraded areas were along segments 118, 170, and 264.

Visual Assessment Figures 15 and 16 visually present the results of the stream assessments. Figure 15 displays the scores for each of the assessed segments. A table of sub-scores and overall scores for each segment is presented on the map.

Figure 16 assigns visual assessment scores to unassessed segments that ranked either "fair" or "poor" in the remote sensing assessment and were similar to assessed segments with respect to near bank soil erodibility, upstream land use, rate of upstream land use change, and slope. Segments that ranked "good" or "excellent" in the remote sensing assessment are also indicated on Figure 16, but were not assigned visual assessment scores.

Figure 15: Visual Assessment Rankings

Figure 16: Visual Assessment Rankings by Remote Sensing Groups

Figure 17: Stream Segments Selected for Visual Assessments from Windshield Survey

Section 6 – Summary of Task 7: Grab Sampling Data Analysis

Task 7: Grab Sampling Data Analysis

This section presents the results of our evaluation of grab sampling data for the 62 square mile Manasquan River Watershed study area. Eighty-four (84) grab samples were collected from seven (7) sampling sites. The samples were analyzed for turbidity, total suspended solids (TSS), and total phosphorus (TP) by New Jersey state certified labs. A Microsoft® Access database with flow, precipitation and water quality analysis results is included in the Appendix B1. Using SAS Institute's JMP® statistical discovery software, linear models were developed using the resulting dataset to assess utility of turbidity monitoring as a surrogate for predicting total phosphorus, and TSS concentrations; to assess the range of concentrations of TSS, turbidity, and TP throughout the watershed; and to describe patterns of spatial and temporal variation.

Methods

Detailed grab sampling guidance was prepared in February 2006 by F. X. Browne, Inc. for AVOCA Engineers and Architects, LLC. to use in the field. The guidance was prepared for and presented to the New Jersey Water Supply Authority in February 2006 (see Appendix C).

Sampling Location Selection

Seven sampling locations were selected on major tributaries or at land use changes draining to the Manasquan River as shown in Figure 20. Sampling locations were selected with accessibility and property owners in mind. Field Technicians were advised to contact property owners to clear access issues. They were also advised to collect samples approximately 200 feet upstream from any bridges or other obstructions whenever possible.

Grab Sampling Analysis

A total of 84 samples were collected from seven different locations between April 2006 and October 2006. Seventy (70) of the eighty-four (84) proposed samples were collected during stormflow conditions. The remaining fourteen (14) samples were collected during baseflow conditions. Grab samples were conducted per the guidance document.

Table 18: Sampling Site Locations and Observations by Test Parameter

		Number of Observations (N)		
Site Name/number	Site Location	TP	TSS	Turbidity
1	Manasquan River @ Georgia Rd.	12	12	12
2	Manasquan River @ Pointe of Woods Dr & Bergerville Rd.	12	12	12
3	Yellow Brook @ Adelphia-Farmingdale Rd.	12	12	12
4	Manasquan River @ Preventorium Rd.	12	12	12
5	Marshes Bog Brook @ Yellow Brook Rd.	12	12	12
6	Mingamahone Brook @ Allaire Rd.	12	12	12
7	Manasquan River @ Hospital Rd.	12	12	12
	All Sites	84	84	84

*See Sampling Location Map (Figure 20) for site locations.

Standardized data were compiled into a Microsoft Access database and information was separated into four tables (organization, parameters, sites, and water quality). Using Access' query and pivot-table functions, TSS and Turbidity data were queried and imported into SAS Institute's JMP software to perform statistical analyses (e.g., ANOVA, multiple regressions, etc.).

Data Analysis

Data were also classified by season, using June 20 and December 20 as start dates of summer and winter respectively, and September 21 and March 21 as start dates of fall and spring, respectively.

A method using the JMP software that involves plotting correlation matrices and calculating Mahalanobis-distances for both TP vs. Turb and TSS vs. Turb was employed to identify outliers in the grab sampling data. This was accomplished in essentially two steps. Firstly, the variables under review are transformed using the Multivariate scatter plot function of the JMP software which plots the data points in a covariance matrix and draws an ellipse around the 95% confidence interval around the correlated points. The narrower the ellipse the more closely correlated the data points are. We then used these scatter plots as a first filter to identify sample sites that are affected by outliers. The JMP software's outlier analysis function which employs a Mahalanobis distance calculation was subsequently performed on those sample sites that exhibited wide ellipses or data points lying at a significant distance outside of the ellipse (Robinson et. al, 2005)..

The second step of this outlier analysis is the calculation of Mahalanobis distance which can be defined as dissimilarity measure between two random vectors $\vec{x}$ and $\vec{y}$ of the same distribution with the covariance matrix Σ:

$$d(\vec{x},\vec{y}) = \sqrt{(\vec{x}-\vec{y})^T \Sigma^{-1} (\vec{x}-\vec{y})}.$$

The Mahalanobis distance calculation helps us to identify true outliers by eliminating the influence of the outlying points on means, averages, and standard deviations and shows points that are most dissimilar to the correlated data points. Observations with an equal

Mahalanobis-distance generally lie on the ellipse. The Mahalanobis-distance is small for observations lying on or close to the principal axis of the ellipse. A point that has a greater Mahalanobis distance from the rest of the sample population of points is said to have higher leverage since it has a greater influence on the slope or coefficients of the regression equation (Robinson et. al, 2005).

Suspicious data points identified by large Mahalanobis distances are then examined to see if excluding them from the regressions will alter the R^2 values. In all cases where an outlier analysis was performed on the Manasquan Watershed dataset, there would be two (2) points identified with large Mahalanobis distances for each sample site. One of these points would usually be the highest result from the largest storm we sampled and the other data point would be an outlier. To determine which data point was the true outlier, each point was excluded and the regression was rerun to examine the R^2 values. Excluding the outlier would improve the R^2 values, but if the other point was excluded, R^2 values would drop significantly.

A stepwise regression procedure was used to construct a series of linear models. In the stepwise regression, factors were considered significant at the $\alpha = 0.05$ level. In the first series of model runs, turbidity, site, season and discharge were used to predict values of TSS and TP. In the second series of model runs, site, season, and discharge were used as predictors of TSS, TP, and turbidity. For all model runs, interaction effects between categorical variables, site, and season, were also evaluated. Standard residual plots were reviewed for trends in variance and normality, and to determine if the mean of the residuals was zero. Data were log-transformed if needed to meet standard assumptions concerning the distribution of residuals. Standard ANOVA tables were generated. F tests were performed for the entire model and for individual variable effect tests. Results from all JMP statistical analyses including the outlier analyses and stepwise regressions are included in Appendix B2.

Results

Hydrograph Analyses

Table 19 summarizes hydrologic data, including the daily peak discharge as observed from the U.S. Geological Survey gauge station of the Manasquan River at Squankum, and the cumulative precipitation as measured at the Howell Weather Station for the ten (10) storm samples and two (2) baseflow samples. Figure 2 shows the magnitude of the stream flow and the distribution of the samples with respect to the sampling time. Of the ten (10) sampling events, five (5) were collected during the receding limb of the hydrographs, three (3) were collected at or near the peak of the storm and the remainder collected during the rising limb of the storm hydrograph. The sampled storms had a range of peak discharge from 65 to 1140 CFS with storm durations ranging from 4-6 hours up to several days before reaching a stable baseflow. The largest storm event sampled was collected after the remnants of Hurricane Ernesto passed through the region.

Table 19: Hydrologic Summary of Sampled Storms

Date	Cum. Precip, in	Peak Discharge (Q), cfs	Location on Main Stem Hydrograph
4/12/2006	0.00	55.00	Baseflow
5/12/2006	0.98	190.00	rising
7/22/2006	0.25	91.00	falling
8/26/2006	1.11	213.00	falling
9/3/2006	3.04	1310.00	peak
9/5/2006	3.04	87.00	falling
9/21/2006	0.00	49.00	Baseflow
10/12/2006	0.84	455.00	peak
10/14/2006	0.84	65.00	falling
10/17/2006	0.93	108.00	rising
10/18/2006	0.93	300.00	falling (near peak)
10/28/2006	1.20	503.00	peak

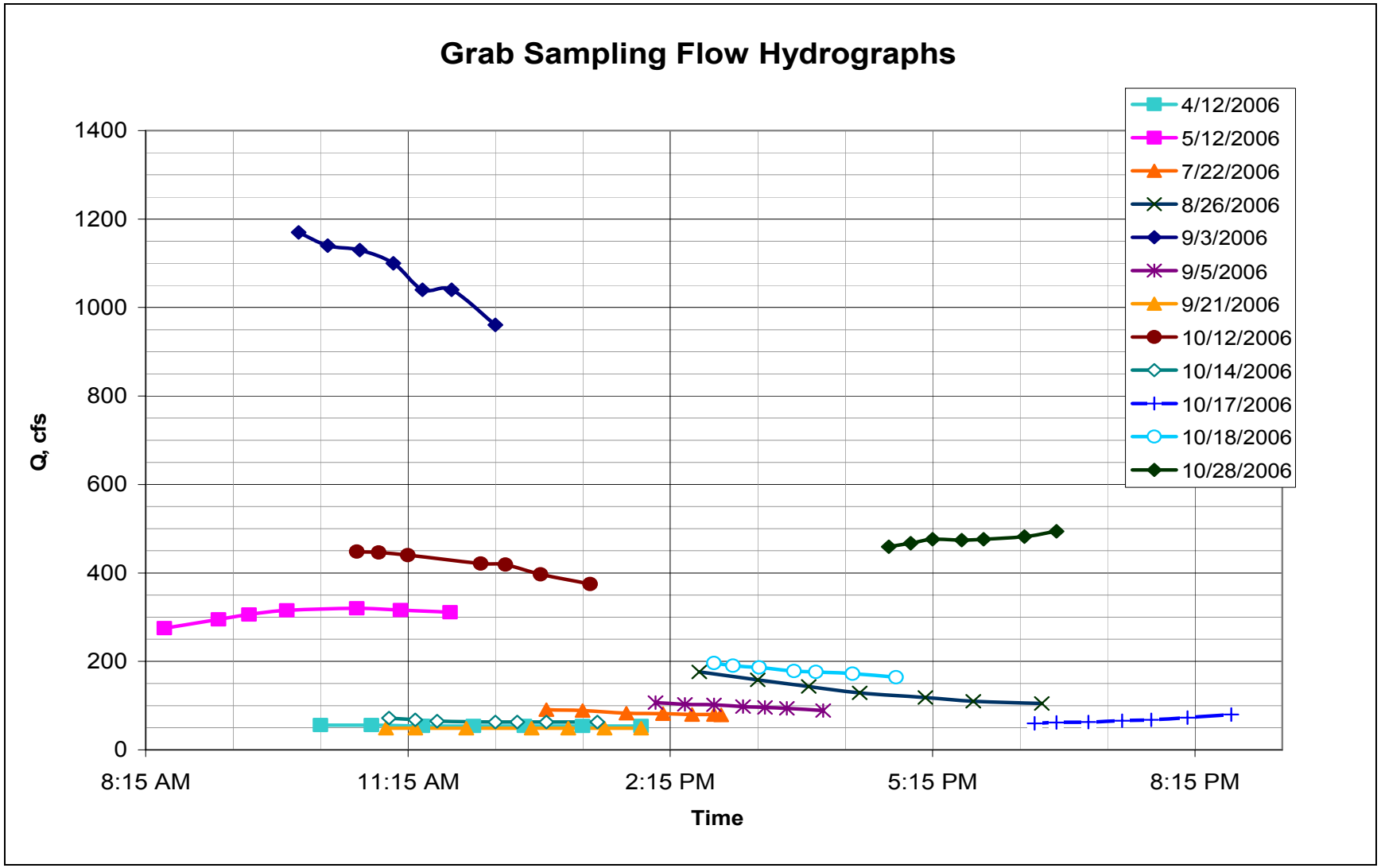

Figure 18: Hydrograph distribution of sampled storms

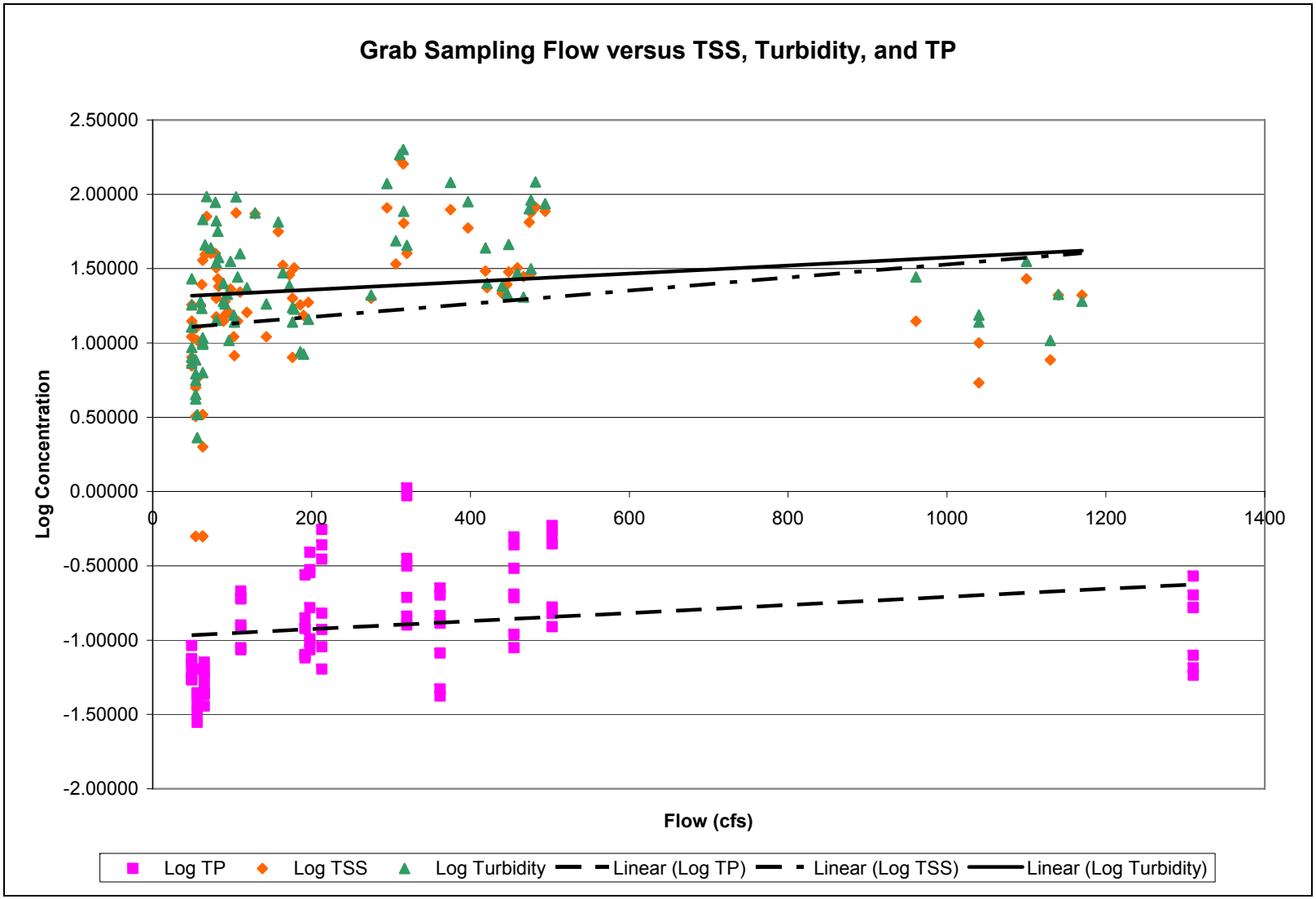

Figure 19: Grab Sampling Flow versus TSS, Turbidity, and TP

Evaluation of Results

Tables 20, 21, and 22 below present a summary of statistics from the analyses of the eighty-four (84) grab samples collected from the study area. To further understand the relationship among parameters, as well as the effect of sampling station (location) and season on parameter values, five linear models were fitted to the dataset using a step-wise linear regression analysis in JMP. The results of the JMP statistical analyses are included in Appendix B2.

Results from the analyses of grab samples collected between April and October 2006 indicates some clear trends. For all parameters, samples collected from locations on the main stem of the Manasquan River generated higher average values than samples collected from sites located on the tributaries with the exception of Site 1, located at the headwaters of the Manasquan River. Also, for the main stem samples, the water quality parameter results tended to increase from the headwaters downstream through the watershed.

As shown in Table 20, turbidity values ranged from 2.3 to 200 NTU, with an average across the entire study area of 36.8 NTU. Site 4, which is located on the Manasquan River downstream of the Howell Middle School, had the highest average turbidity results, while Site 5 and Site 1 had the lowest average turbidity results. Site 3 also had relatively low turbidity results and the lowest turbidity result was generated from a sample obtained from Site 3. Site 1 is located at the headwaters of the Manasquan River and its drainage area is dominated by the Turkey Swamp wildlife management area. Sites 3 and 5 are both tributaries to the Manasquan River whose subwatersheds are also undeveloped and are dominated by open space and small agricultural land uses.

Table 20: Turbidity Summary Statistics for Grab Sample Analyses

Site	Sampling Location	Turbidity (NTU)			
		Min	Max	Mean	St. Dev
1	Manasquan River @ Georgia Rd.	3.3	80.0	23.4	20.7
2	Manasquan River @ Pointe of Woods Dr & Bergerville Rd.	2.3	118.0	43.4	39.5
3	Yellow Brook @ Adelphia-Farmingdale Rd.	4.5	67.7	24.2	19.0
4	Manasquan River @ Preventorium Rd.	4.2	200.0	59.0	56.3
5	Marshes Bog Brook @ Yellow Brook Rd.	6.2	45.3	18.5	11.9
6	Mingamahone Brook @ Allaire Rd.	7.7	88.2	32.1	26.4
7	Manasquan River @ Hospital Rd.	5.6	185.0	56.8	55.5
Overall		**2.3**	**200.0**	**36.8**	**38.6**

Table 21 shows TSS values ranging from 0.5 to 173 mg/L, with an overall average of 28.7 mg/L. Site 4 also had the highest average TSS concentrations of all sampling locations. Sites 3 and 5 produced the lowest average TSS concentrations and reflected the trends seen with turbidity. Results for TP as summarized in Table 22 showed TP values ranging from 0.028 to 1.056 mg/L with an average of 0.185 mg/L. Site 4 again produced the highest average TP concentrations of all sampling locations. The lowest concentrations of TP were obtained from Site 3, and 5. These sampling locations are all located on tributaries to the Manasquan River and the results show the same trends discussed above.

Table 21: TSS Summary Statistics for Grab Sample Analyses

Site	Sampling Location	Total Suspended Solids (mg/L)			
		Min	Max	Mean	St. Dev
1	Manasquan River @ Georgia Rd.	3.3	64.7	22.5	16.6
2	Manasquan River @ Pointe of Woods Dr & Bergerville Rd.	0.5	81.0	33.2	29.3
3	Yellow Brook @ Adelphia-Farmingdale Rd.	2.0	36.0	19.2	10.4
4	Manasquan River @ Preventorium Rd.	0.5	160.0	44.4	44.9
5	Marshes Bog Brook @ Yellow Brook Rd.	0.5	40.0	16.5	11.1
6	Mingamahone Brook @ Allaire Rd.	0.5	64.0	20.5	18.8
7	Manasquan River @ Hospital Rd.	0.5	173.0	44.3	49.7
Overall		**0.5**	**173.0**	**28.7**	**30.8**

Table 22: TP Summary Statistics for Grab Sample Analyses

Site	Sampling Location	Total Phosphorus (mg/L)			
		Min	Max	Mean	St. Dev
1	Manasquan River @ Georgia Rd.	0.064	0.444	0.169	0.107
2	Manasquan River @ Pointe of Woods Dr & Bergerville Rd.	0.043	0.449	0.204	0.139
3	Yellow Brook @ Adelphia-Farmingdale Rd.	0.042	0.165	0.084	0.041
4	Manasquan River @ Preventorium Rd.	0.028	0.935	0.316	0.258
5	Marshes Bog Brook @ Yellow Brook Rd.	0.036	0.354	0.101	0.086
6	Mingamahone Brook @ Allaire Rd.	0.037	0.315	0.119	0.078
7	Manasquan River @ Hospital Rd.	0.033	1.056	0.299	0.305
Overall		**0.028**	**1.056**	**0.185**	**0.187**

Turbidity Effects

Grab sampling data were analyzed to determine if turbidity could be used as a predictor of TSS and TP. SAS Institute's JMP statistical software was employed to generate linear regression models for each site to determine if turbidity and TSS were at all correlated. Table 23 clearly shows a significant relationship between TSS and turbidity ($\acute{\alpha} < 0.0001$) for all sampling locations with very good model fit ($R^2 = 0.933$). The relationship between TSS and turbidity is significant for each individual site as well, ($\acute{\alpha}$ ranges from < 0.0001 to 0.0005) and the model fit is also strong (R^2 ranges from 0.733 to 0.964).

Table 23: TSS/Turbidity Correlations by Site

Site Number	Site Name	Observations (n)	R^2 Adjusted	Probability (ά)
1	Manasquan River @ Georgia Rd.	12	0.861	<0.0001
2	Manasquan River @ Pointe of Woods Dr & Bergerville Rd.	12	0.964	<0.0001
3	Yellow Brook @ Adelphia-Farmingdale Rd.	11*	0.779	0.0002
4	Manasquan River @ Preventorium Rd.	12	0.951	<0.0001
5	Marshes Bog Brook @ Yellow Brook Rd.	11*	0.733	0.0005
6	Mingamahone Brook @ Allaire Rd.	11*	0.831	<0.0001
7	Manasquan River @ Hospital Rd.	12	0.935	<0.0001
Overall		**81****	**0.933**	**<0.0001**

* one (1) outlier excluded from analysis
** three (3) outliers excluded from analysis

Table 24 indicates an equally significant relationship between TP and turbidity (ά < 0.0001) for all sampling locations with very good model fit (R^2 = 0.913). TP and turbidity relationships at the site level were also significant (ά < 0.0001). The model fit for each site model was also very strong (R^2 ranges from 0.877 to 0.951).

Table 24: TP/Turbidity Correlations by Site

Site Number	Site Name	Observations (n)	R^2 Adjusted	Probability (ά)
1	Manasquan River @ Georgia Rd.	12	0.924	<0.0001
2	Manasquan River @ Pointe of Woods Dr & Bergerville Rd.	11*	0.900	<0.0001
3	Yellow Brook @ Adelphia-Farmingdale Rd.	12	0.877	<0.0001
4	Manasquan River @ Preventorium Rd.	12	0.951	<0.0001
5	Marshes Bog Brook @ Yellow Brook Rd.	11*	0.881	<0.0001
6	Mingamahone Brook @ Allaire Rd.	11*	0.931	<0.0001
7	Manasquan River @ Hospital Rd.	12	0.929	<0.0001
Overall		**81****	**0.913**	**<0.0001**

* one (1) outlier excluded from analysis
** three (3) outliers excluded from analysis

These strong correlations provide further support for using turbidity as a surrogate for TSS and TP to estimate sediment and phosphorus loading within the study area.

Site, Season and Discharge Effects

Table 25 summarizes the effects of site location, seasonal variation and discharge on the TSS, Turbidity and TP. All models were assessed for site, season, discharge and interaction effects between these predictors. All effects that did not yield significant results were excluded and the analysis reran to narrow down the significant predictors. These results indicate that there are significant site, season and discharge effects on the water quality parameters. Seasonal variation and discharge have a significant effect on all three parameters analyzed as shown in the first three rows of Table 25 ($\acute{\alpha} < 0.0001$). TP values are also significantly affected by the location of the site. Examining the dataset closely, seasonal variation and discharge are closely linked. Storms with the greatest peak discharges were sampled in the summer and the fall. Discharge did not have a significant effect on the TSS/Turbidity relationship ($\acute{\alpha} = 0.4471$). The seasonal effect or the strength of Turbidity as a predictor may have masked the effect of discharge on this relationship. The effect of site location on TP values may be a direct result of differing land uses at the different sites. Evaluating these effects with turbidity as a predictor of TSS and TP, the regressions show that a very strong correlation exists between Turbidity and TSS and that only seasonal variation has a significant effect on this model ($R^2 = 0.787$, $\acute{\alpha} < 0.0001$). Since seasonal variation and peak discharge are so closely related in the grab sampling dataset, it is difficult to eliminate discharge as an effect on this correlation. The fact that discharge has an effect on both turbidity and TSS when evaluated separately would seem to strongly indicate that the effect of discharge has likely been incorporated in the effect of seasonal variation. The regression analysis of turbidity and TP with these effects tests clearly shows that turbidity is strongly correlated with TP ($R^2 = 0.865$) and that the effect of discharge on turbidity ($\acute{\alpha} < 0.0001$) plays a major role in this correlation.

Table 25: Regression Analyses with Test Effects

Significant Predictor (X):	Response (Y):	Regression Type	Modifications	Adjusted R^2	Probability ($\acute{\alpha}$)
log(TURB), season	log(TSS)	Stepwise	outliers excluded	0.787	<0.0001
season, discharge, discharge*season	log(TSS)	Stepwise	outliers excluded	0.355	<0.0001
season, discharge	log(TURB)	Stepwise	outliers excluded	0.341	<0.0001
log(TURB), site, log(TURB)*discharge	log(TP)	Stepwise	outliers excluded	0.865	<0.0001
site, season, discharge, discharge*season	log(TP)	Stepwise	outliers excluded	0.431	<0.0001

Upstream Land Use Effects

To further understand the results of the model with respect to sampling locations, the mean values of each parameter at each sampling location were correlated to upstream land use. The results of this correlation analysis are summarized below in Table 26 and included in Appendix B3. Although effects tests were not performed, visual inspection of the correlation graphs shows that there are no significant correlations between the site means of the parameters and upstream land use.

Table 26: Upstream Land Use Correlation Analysis

Significant Predictor (X):	Response (Y):	Regression Type	Modifications	Adjusted R^2	Probability (ά)
% Agriculture	TSS	Least Squares	outliers excluded	0.051	0.0235
% Urban	TSS	Stepwise	outliers excluded	0.074	0.0076
% Ag+Urban	TSS	Stepwise	outliers excluded	0.072	0.0085
% Agriculture	TP	Stepwise	outliers excluded	0.106	0.0017
% Urban	TP	Stepwise	outliers excluded	0.147	0.0002
% Ag+Urban	TP	Stepwise	outliers excluded	0.143	0.0003

Table 26 summarizes correlations with upstream land use and indicates that the upstream land use does significantly affect TP, and TSS values. Both the percentage of agriculture and the percentage of urban land use upstream of the sampling locations significantly affect TSS values (ά = 0.0235 and ά = 0.0076, respectively). TP values are also significantly affected by upstream land use (ά = 0.0017 for agriculture and ά = 0.0002 for urban). For both parameters, TP and TSS, the percentage of upstream urban land use appears to have a greater influence on the model. However, as the results summarized in Table 26 indicate, the upstream land use alone does not explain the variability within the data set and results in poor model fits for both TP ($0.106 \leq R^2 \leq 0.147$) and TSS ($0.051 \leq R^2 \leq 0.074$).

Data and Analysis Limitations

The majority of grab samples were collected during the summer and fall months with the largest storm event occurring in the summer. Therefore, the effect of seasonal variation on the parameters may be skewed towards summer and to a lesser extent, the fall. The models show that discharge has a clear effect on the parameters but the fit of the models are not improved by having discharge as an additional predictor. The discharge values were obtained from the USGS gauge station at Squankum which is downstream of site 4. Sites 3, 5 and 6 are located on tributaries to the Manasquan River and the discharge from the drainage areas to those sampling locations do not correlate as closely to the gauge station at Squankum. Likewise, the smaller drainage areas of the upstream sampling locations at Sites 1 and 2 would also correlate poorly with the gauge station. The smaller drainage areas associated with tributaries and upstream sampling

sites translates into smaller peak rates of runoff due to a smaller volume of runoff. The smaller drainage areas also results in shorter times of concentration and these peak rates occur earlier in the hydrograph than downstream sites such as the USGS gauge station at Squankum. Also, many of the grab samples were collected during the peak flow or at the receding limb of the hydrograph for the main stem of the Manasquan River. Despite these limitations, it is evident from the results that discharge affects all of the parameters. These results also seem to indicate that turbidity may be an appropriate surrogate to estimate the quantity of TSS and TP present within the Manasquan River watershed.

Figure 20: Grab Sampling Site Map for AVOCA Associates

Section 7 – Summary of Task 4: Continuous Water Quality Monitoring

Task 4: Continuous Water Quality Monitoring

This section presents the results of our evaluation of continuous monitoring data for the 62 square mile Manasquan River Watershed study area. Automated water quality monitoring stations were set up at seven (7) sampling sites as shown on Figure 21: Automated Water Quality Monitoring Stations. YSI Inc. 600-OMS multiparameter sondes were used to continuously sample water temperature, turbidity, depth and specific conductance at ten (10) minute intervals. On a biweekly basis, the sondes were recalibrated, had their batteries changed and water samples were collected at the locations of the automated water quality monitoring stations. The grab samples were then delivered to the laboratory at the NJWSA intake facility in Wall Township, NJ and to J. R. Henderson Labs for analysis, including turbidity, total iron, pH, and apparent and true color. Field measurements of water temperature, pH and ferrous iron were also conducted at the same time as the grab sampling and sonde maintenance.

Methods

Detailed grab sampling guidance was prepared in February 2006 by F. X. Browne, Inc. for AVOCA Engineers and Architects, LLC. to use in the field. The guidance was prepared for and presented to the New Jersey Water Supply Authority in February 2006 (see Appendix C). The YSI 6-series multiparameter water quality sondes user manual and assistance from technical representatives of YSI Incorporated were employed to set up and calibrate the sondes in the field. Ferrous Iron was analyzed using the LaMotte Smart Spectro portable spectrophotometer and field kits. The ferrous iron field kits utilized the APHA 3500-FE Iron B – 1,10 Phenanthroline colorimetric method for measuring trace quantities of iron in water samples.

Sampling Location Selection

Seven sampling locations were selected on major tributaries or at land use changes draining to the Manasquan River as shown in Figure 21. Sampling locations were selected with accessibility and property owners in mind. Field Technicians were advised to contact property owners to clear access issues. Site 7, originally located at the NJWSA intake facility on the Manasquan River was relocated to Debois Creek to further characterize the headwaters region in the northeastern portion of the watershed. A USGS gauge station installed with automated turbidity monitoring equipment at the NJWSA intake facility made installing a monitoring station at that location redundant. Site 4 was also relocated upstream towards the crossing of Southard Avenue due to anomalous results recorded during the grab sampling task and field observations of possible increased runoff coming from the adjacent Howell Middle School..

Data Collection and Processing:

Data was retrieved from the memory modules of each individual sondes on a biweekly basis during regular calibration and maintenance. These calibration and data download dates were noted beforehand and the data was examined manually during those dates when the sonde was physically removed from the sampling location. We excluded those points from the summary statistics wherever that occurred. Outliers such as extremely high data points in the turbidity data were also examined and excluded. We based the decision of which high points to exclude on the values obtained from the analysis of

samples obtained in the grab sampling performed in the previous tasks (i.e. knowing what size storm correlates to the expected peak turbidity value) and also on the graph of the data points. Generally, we noticed that the high turbidity points will be greatly separated from the main curve of the data points and it was usually pretty clear that they were outlier points. Outlier points on the depth curves were similarly filtered out but with depth values the opposite was the case, we had to filter or adjust the low points. Using AVOCA Engineers and Architects' firsthand knowledge of actual flow conditions in the field that even at the lowest flow conditions the sondes remained covered with water, we assumed that the base flow at all sites should not fall below 0.025 meters. We examined the data and noticed that the low points occurred after sonde units were removed from the water and typically took some time to readjust. We used the assumption of the field observed lowest flow and the general shape of the depth curves to readjust the period immediately after recalibrations. These curves were then visually compared to the stage data at USGS gauge stations before the data was summarized.

Data Analysis:

Due to the quantity of data obtained from the continuous monitoring program, analyzing data using statistical models as was performed in previous tasks proved to be prohibitive and counter-productive. Instead, the data was processed and reduced as detailed above and summary statistics were calculated as summarized in the tables below.

An analysis of storm travel times was performed using the depth curves from the sonde units based on the rainfall event data of the Howell Weather Station. Travel time was calculated from the leading edge of the rising limb of the hydrograph to the point where it returned to that initial depth. The time to peak was calculated from that initial base point on the rising limb to the peak value. An examination of tributary and main-stem hydrographs was also performed utilizing both the leading edge and peak discharge points. The results of these calculations are also provided in Appendix E.

Results:

Table 27: Automated Water Quality Monitoring Stations by Month

	Temperature, degrees C			Conductivity, mS/cm			Depth, meters			Turbidity, NTU		
	Min	Max	Mean	Min	Max	Mean	Min	Max	Mean	Min	Max	Mean
April	9.13	18.49	13.72	0.074	0.354	0.188	0.059	1.777	0.583	N/A	N/A	N/A
May	8.74	21.72	15.34	0.092	0.517	0.215	0.039	1.225	0.461	N/A	N/A	N/A
June	12.76	23.65	18.31	0.085	1.008	0.225	0.039	1.543	0.371	N/A	N/A	N/A
July	13.72	24.65	19.91	0.054	0.525	0.227	0.032	1.956	0.344	4.5	579.4	31.2
August	15.74	25.43	19.81	0.065	0.582	0.228	0.027	1.000	0.266	5.6	346.6	24.7
September	11.47	23.69	17.45	0.084	0.317	0.242	0.021	0.579	0.200	3.6	420.1	20.5
October	7.12	21.33	15.39	0.103	0.557	0.247	0.025	0.871	0.321	2.0	420.1	20.1
November	2.26	13.99	8.20	0.100	0.340	0.222	0.001	0.738	0.354	2.5	268.9	14.9

Table 28: Automated Water Quality Monitoring Stations by Site

	Temperature, degrees C			Conductivity, mS/cm			Depth, meters			Turbidity, NTU		
	Min	Max	Mean	Min	Max	Mean	Min	Max	Mean	Min	Max	Mean
Site 1	2.26	24.65	15.39	0.054	0.525	0.219	0.001	0.857	0.208	2.50	284.60	22.01
Site 2	3.88	25.15	16.43	0.075	0.401	0.267	0.027	1.956	0.545	3.20	579.40	19.89
Site 3	7.27	22.33	15.85	0.119	0.216	0.180	0.025	0.633	0.372	n/a	n/a	n/a
Site 4	5.41	23.39	15.73	0.120	0.582	0.274	0.037	1.576	0.411	2.00	449.70	29.60
Site 5	3.27	24.57	16.12	0.065	0.277	0.162	0.021	0.714	0.308	n/a	n/a	n/a
Site 6	3.69	23.91	16.14	0.086	0.371	0.173	0.219	1.264	0.603	4.50	192.50	33.77
Site 7	3.23	25.43	16.73	0.062	1.008	0.295	0.039	1.468	0.513	3.40	325.40	22.03
Overall	**2.26**	**25.43**	**16.02**	**0.054**	**1.008**	**0.224**	**0.001**	**1.956**	**0.479**	**2.00**	**579.40**	**25.46**

As shown in Table 28, there was a loss of turbidity data during the first three months of the automated monitoring program. This was due to silt and sediment being carried into the multiparameter sondes and blocking the optical lens of the turbidity probes. With the help of YSI field representatives, this problem was remedied in July and turbidity measurements were obtained for the rest of the monitoring program. Table 28 also shows that turbidity measurements at Sites 3 and 5 were not available. Silt and sedimentation continued to interfere with the optical lens at sites 3 and 5. The probes at these two sites had to be removed and turbidity data is not available for these two locations.

Table 29: pH and Ferrous Iron Field Measurements by Month

	pH			# of Samples	Ferrous Iron, ppm			# of Samples
	Min	Max	Mean		Min	Max	Mean	
May	5.46	7.04	6.42	3	1.17	6.98	3.31	2
June	5.96	7.13	6.73	2	2.00	6.16	3.80	2
July	6.32	7.22	6.77	2	1.16	6.26	3.07	2
August	6.43	7.28	6.83	2	0.83	5.16	3.27	2
September	-	-	7.04	1	-	-	2.14	1
October	6.52	7.47	7.04	2	-	-	2.57	1
November	6.54	7.70	7.13	4	0.99	6.60	2.90	4

In addition to data obtained from the automated water quality monitoring stations, field measurements of pH and ferrous iron were taken during biweekly calibration and maintenance visits to the automated water quality monitoring stations. Due to short holding times for both pH and ferrous iron, these measurements were taken in-situ with a portable pH meter and portable LaMotte spectrophotometer and iron test kits. PH and ferrous iron measurements were taken to help the NJWSA determine a source for the presence of a reddish-orange coloration in the surface waters draining to the NJWSA intake facility. Data for these two parameters are summarized in Tables 29 and 30. A shortage in ferrous iron test kits prevented measurements during September and October where there was only one measurement of ferrous iron for those months.

Table 30: pH and Ferrous Iron Field Measurements by Site

	pH			# of Samples	Ferrous Iron, ppm			# of Samples
	Min	Max	Mean		Min	Max	Mean	
Site 1	5.46	7.70	6.73	16	2.14	5.14	3.11	14
Site 2	6.42	7.41	6.97	16	0.83	2.80	1.62	14
Site 3	6.23	7.01	6.75	16	3.87	9.64	5.30	14
Site 4	6.67	7.47	7.16	16	1.80	3.76	2.47	14
Site 5	5.53	6.92	6.38	16	1.63	6.16	3.29	14
Site 6	6.72	7.40	6.99	16	1.91	5.40	3.71	14
Site 7	6.33	7.39	6.98	16	0.90	2.42	1.56	14

Evaluation of Automated Water Quality Monitoring Data:

Temporal Variations

Examining Table 27 which portrays the effect of temporal variation on the data, there are several trends that should be noted. The temperature data clearly shows that as the ambient air temperature rises and falls with the change in seasons, the water temperature is similarly affected.

Specific Conductance and Turbidity values are both higher in the summer months of June-August, with average values highest in July. Maximum values of specific conductance and depths however appear to peak earlier in the months of spring. It is reasonable to assume that the higher flows associated with snowmelt and spring rains would also lead to higher maximum values of turbidity. Higher precipitation amounts and larger volumes of runoff flow leads to larger amounts of sediment being washed off into surface waters during each storm event. During the dryer conditions of summer months, there are larger gaps between discrete storm events. These dry periods allow for sediment to build up on pavement and other impervious surfaces and therefore a greater amount of sediment to potentially be washed off into surface waters than is evident during wetter spring months. Reduced base flow with dissolved iron from the glauconitic soils could also be a cause for increased turbidity. Additionally, summer is the time of year when storm events tend to be flashier, meaning higher rain intensities, which also can cause more sediment to be washed into, or re-suspended from sediment deposition to the surface waters. These trends are reflected in the higher average values of both specific conductance and turbidity values measured by the automated monitoring stations during the summer.

The automated monitoring station data trends even lower during the fall months when compared to data from spring and summer months. Values on average tended to dip as the temperatures started to cool off from their peak in July and as flow as reflected in the depth measurements began to taper off, the lowest values of turbidity and specific conductance were recorded.

Spatial Variations

Table 28 summarizes the automated water quality monitoring data by site location. The data demonstrates some notable trends with respect to spatial variations captured by the

monitoring stations. Sites 1, 2 and 4 are all located on the main stem of the Manasquan River, with site 1 being farthest upstream and site 4 being farthest downstream. Sites 3, 5, 6 and 7 are all located on major tributaries, of which site 7 is located in the most urbanized and developed part of the watershed, site 3 in the least developed part of the watershed and the other two in moderately developed portion of the watershed. Values for both turbidity and specific conductance tended to increase downstream along the main stem sites. On average values for these parameters also tended to be higher on the main stem than on the tributary sites. Of the tributary sites, site 7 generally had higher values for turbidity and specific conductance. Sites 3 and 5 had the lowest specific conductance values of any site. Specific conductance is a measurement of a solution to pass an electric current and in water is affected by the presence of inorganic dissolved solids. Low conductivity values indicate a lower amount of dissolved ions that could potentially coagulate suspended and colloidal particles that contribute to turbidity. . Drainage areas to sites 3 and 5 are relatively undeveloped and in generally good health according visual assessments. The low specific conductance values may be an indication of lower concentrations of trace metals being washed off into these surface waters. Lower amounts of dissolved ions at these sites may be lowering the capability of these waters to buffer turbidity and remove suspended and colloidal particles. The highest values for turbidity and specific conductance were measured at sites 2 and 7 where highly developed landscape, increased imperviousness and the presence of highly erodible soils may be contributing to elevated levels of sediment and suspended solids and wash off trace metals into the surface waters.

Table 31:: Upstream Land Use/Land Cover to Monitoring Stations

Site Number	Site Name	% Ag	% Urban	%Ag+Urban
1	Manasquan River @ Georgia Rd.	16.8%	32.3%	49.1%
2	Manasquan River @ Pointe of Woods Dr & Bergerville Rd.	18.3%	49.6%	67.9%
3	Yellow Brook @ Adelphia-Farmingdale Rd.	11.7%	17.1%	28.8%
4	Manasquan River @ Southard Ave.	18.9%	42.6%	61.5%
5	Marshes Bog Brook @ Yellow Brook Rd.	3.8%	16.9%	20.7%
6	Mingamahone Brook @ Allaire Rd.	6.3%	21.7%	28.0%
7	Debois Creek @ Halls Mill Rd.	11.3%	13.7%	24.9%
8	Manasquan River @ Hospital Rd.	12.5%	32.3%	44.8%

Evaluation of In-Situ Field Measurements:

pH

In-situ field measurements at the seven (7) automated water quality monitoring stations showed that overall, the Manasquan River exhibited near-neutral pH. On average pH values for sites 1, 3, and 5 are slightly more acidic than the other sites. Drainage areas to these three locations are the least developed areas within the entire watershed, particularly sites 1 and 3. pH was highest at sites 4 and 6 which were the most downstream locations in the watershed.

The trend in the pH measurements with respect to temporal variation was a steadily increasing one. The average values across all the sites trended upwards from May to

November. Precipitation is generally more acidic than waters in natural streams and higher amounts of rainfall during the spring, in addition to lime applications on agricultural fields and lawns, may explain the upward trend in pH.

Ferrous Iron

In-situ field measurements at the seven (7) automated water quality monitoring stations showed that overall the surface waters within the Manasquan watershed average around 3 ppm. Sites with mostly undeveloped or natural drainage areas such as sites 1, 3, 5 and 6 generally have significantly higher values than the other sites, both on average and with maximum values. Sites 2 and 7 with the most developed drainage areas in turn had the lowest values for ferrous iron.

Ferrous iron values also tended to be higher during the summer months, peaking in June and falling off steadily into the autumn. The lowest values appeared to be measured during September and October; however, measurements were limited during those months due to shortages in iron test kits and supplies. Based on the measurements in the adjacent months, it is reasonable to assume that ferrous iron values are lower in these early autumn months.

Figure 21: Automated Water Quality Monitoring Stations

Section 8 – Project Assessment and Results

Project Assessment and Results

This section combines the review and analysis of the four previous tasks. The tasks reviewed were watershed modeling, remote sensing data, visual assessment and water quality monitoring. By comparing and contrasting all previous tasks, a recognizable pattern was developed that detailed the most significant sources of sediment loading to the Manasquan River. Twenty locations were identified that exhibited the most severe deposition of silt and had the highest likelihood of success in lowering the levels of Total Suspended Solids (TSS), Turbidity (Tu) and Total Phosphorous (TP). These locations were categorized and evaluated for potential mitigation projects.

Evaluation of Results

In Task 1- Assessing Water Quality Data, This project task represents the results of our evaluation of existing water quality data for the 62 sq. mile Manasquan River Watershed study area. Ambient water quality data (total suspended solids (TSS), turbidity, fecal coliform and total phosphorus (TP)) from Monmouth County Health Department (MCHD), New Jersey Water Supply Authority (NJWSA) and New Jersey Department of Environmental Protection (NJDEP) were collected, standardized and organized into a Microsoft Access database. Using JMP software, linear models were developed using the resulting dataset to assess utility of turbidity monitoring as a surrogate for predicting fecal coliform, phosphorus, and TSS concentrations; to assess the range of concentrations of TSS, turbidity, TP, and fecal coliform throughout the watershed; and to describe patterns of spatial and temporal variation.

Results of our existing water quality data review for the study area indicate that turbidity may be an adequate, if not highly accurate predicator of TSS levels in stream water within the Manasquan Watershed. Although bivariate plots revealed several weak and statistically non-significant relationships between TSS and turbidity for individual sites and seasons, based on the overall significance and fit of the full model, we would recommend proceeding with grab sampling collection to develop TSS/turbidity models for use in the project. We can reassess the utility of the turbidity-based modeling approach based on the results of the grab sampling analysis. Our results suggest that turbidity has limited utility as a predictor of fecal coliform or TP concentrations.

Our model results suggest significant spatial differences in TSS, turbidity, and TP concentration throughout the watershed, although obvious explanations for these spatial differences were, for the most part, not evident. TSS concentrations were generally higher in the tributaries draining the north central portion of the watershed in Howell Township and lower in the main stem of the Manasquan River. Many of the former areas are experiencing rapid conversion from agricultural to suburban land uses, which may help to explain the elevated levels. We found the lowest fecal coliform levels at disparate locations; Site 1, located in the headwaters of the watershed in Freehold Township and in Site 15, located in the central portion of the watershed in Howell Township. In both cases, however, the upstream watershed is largely undeveloped and as was shown in Figure 5: Annual Total Suspended Solids Yields from WinSLAMM Modeling, the trend in the study area is for watersheds dominated by urban land use to generate higher values of fecal coliform. We also found relatively low mean levels at Site 6, which is located just downstream of the highly developed portions of Freehold Township and Freehold Borough. It is interesting to note that three very high results for fecal coliform were

recorded at Site 6, but were removed in the outlier analysis. We found the highest TP levels at Site 1 (which also recorded among the lowest fecal coliform levels). Other sites with elevated TP levels were located throughout the watershed without an obvious spatial pattern.

The importance of seasonal variation in fecal coliform, TSS, and turbidity levels may warrant consideration of a longer automated monitoring period in the next phase of the project.

Finally, we must stress the many limitations inherent in both the current data set and the models including insufficient data for flow conditions at the time of sampling, and the variability in analysis methods among datasets. The predictor values should be used with careful consideration or the data set should be expanded so the models can be fine-tuned to reflect more accurate relationships.

FXB determined that there were direct relationships between TSS, Turbidity and TP throughout the watershed. Subwatersheds 2, 4, 5, 6, 7, 9, 21, 23 and 24 had the highest levels. The increase in urbanization and erosive soil types in the western and northwestern part of the watershed has been a major contributor for the TSS and TP.

In Task 2- Watershed Modeling, F. X. Browne Inc. conducted watershed modeling of the Manasquan River Watershed study area using WinSLAMM (ver. 9.0). F. X. Browne, Inc. developed model parameters using existing data available from MRWA, NJDEP, NJWSA, and others. Aerial photography and field reconnaissance were used to verify and refine model parameters and source area delineations. Precipitation data was obtained from the South Jersey Resource Conservation and Development Council and was converted into a WinSLAMM rain parameter file. Land use classifications and watershed delineations used in the Remote Sensing Analysis were used in the WinSLAMM model. Model runs generated annual and unit area adjusted annual loadings for total suspended solids (TSS) and total phosphorus (TP) for each of 24 subwatersheds in the study area.

WinSlamm model results for the Manasquan River Watershed study area indicate that subwatersheds annual TSS loads ranged from 158 to 3,622 tons/year. TSS yields ranged from 0.23 to 0.67 tons/acre/year when normalized by subwatershed area. Annual TP loads ranged from 0.17 to 3.85 tons/year and yields ranged from 0.0003 to 0.0012 tons/acre/year.

Subwatersheds 1, 6, 7, 15, 17, 18 and 21 had the highest annual TSS loads. Subwatersheds 6 and 7 drain the majority of Freehold Borough, one of the more densely populated and developed areas within the study area. Subwatershed 17 is dominated by Naval Station Earle and subwatershed 18 drains most of Farmingdale Borough and the regional airport nearby. Subwatershed 21 is characterized by a sharp increase in the development of residential areas. Subwatershed 1 drains the headwaters of the Manasquan River Watershed and is mostly undeveloped and protected in large part by the Turkey Swamp Wildlife Management Area.

Subwatersheds 1, 5, and 16 produced the highest TSS annual yields. Subwatersheds 5 and 16 are located in transitional regions that are experiencing increased conversion of agricultural lands to residential development.

Subwatersheds 2, 6, 7, 18 and 21 produced the highest annual TP loads, while subwatersheds 2 and 4 produced the highest TP yields. Subwatersheds 2 and 4 both drain highly residential areas in Freehold Township.

In Task 3- Visual Assessments, we used GIS Remote Sensing to calculate a list of sites with potential for contributing high sediment loads. We then conducted a visual assessment of twenty-one (21) reaches throughout the watershed to confirm the remote sensing and rank the stream segments. The stream reaches were ranked, recorded and mapped in GIS. The main types of degradation observed were incision, widening, aggradation and areas of planform changes. The affected areas were along the main stem of the Manasquan, especially on segments 15, 17, 18 and 30.

In Task 4- Screening Water Quality Monitoring, fixed monitoring stations were set up in seven (7) locations. The monitoring stations were inspected every two weeks over a period of six (6) months. Temperature, pH, total iron, ferrous iron, ferric iron and conductivity data was collected. The results were calculated and statistically charted.

Comparison of Results

An analysis of existing water quality data was conducted during Task 1 and the analysis of data from grab sampling at seven (7) sites were analyzed in the same manner. Tables 32 through 34 below compare the summary statistics from these analyses. Summary statistics for turbidity measurements during the automated water quality monitoring phase has been included in Table 32 for comparison as well. TSS and TP were not measured during the automated water quality monitoring phase and cannot be directly compared in the same manner.

Summary Statistics

Table 32: Turbidity Analysis Statistics (NTU)

	Existing Water Quality Data	Grab Sampling Data	Automated Monitoring Data
Min	2.9	2.3	2.0
Max	75	200	579.40
Mean	15.6	36.8	25.46
St. Dev	15.8	38.6	44.8

Table 33: TSS Analysis Statistics (mg/l)

	Existing Water Quality Data	Grab Sampling Data
Min	1.0	0.5
Max	32.0	173
Mean	9.29	28.7
St. Dev	6.90	30.8

Table 34: TP Analysis Statistics (mg/l)

	Existing Water Quality Data	Grab Sampling Data
Min	0.010	0.028
Max	1.810	1.056
Mean	0.203	0.185
St. Dev	0.281	0.187

Linear Models

Results from the step-wise linear regression analyses performed in SAS Institute®'s JMP™ Statistical Discovery Software for both the existing water quality data and data analyzed during the grab sampling analysis of Task 7 are presented in Table 35 below. Fecal coliform was not a parameter measured during the grab sampling phase of the project and therefore no linear regression analysis was performed to evaluate that parameter. Instead an evaluation of turbidity as a predictor of TP was analyzed during the grab sampling phase as reflected in b.) of Table 35 below.

Table 35: Regression Analyses and Statistical Model Summary

a.) Existing Water Quality Data:

Significant Predictor (X):	Response (Y):	Regression Type	Modifications	Adjusted R^2	Probability (ά)
log(TURB), site, season, discharge	log(TSS)	Stepwise	outliers excluded	0.590	<0.0001
site, season, site*season, discharge	log(TSS)	Stepwise	outliers excluded	0.395	<0.0001
site, season, discharge	log(TURB)	Stepwise	outliers excluded	0.444	<0.0001
site, season, discharge	log(FECAL)	Stepwise	outliers excluded	0.414	<0.0001
site, discharge	log(TP)	Stepwise	outliers excluded	0.349	<0.0001

b.) Grab Sampling Data:

Significant Predictor (X):	Response (Y):	Regression Type	Modifications	Adjusted R^2	Probability (ά)
log(TURB), season	log(TSS)	Stepwise	outliers excluded	0.787	<0.0001
season, discharge, discharge*season	log(TSS)	Stepwise	outliers excluded	0.355	<0.0001
season, discharge	log(TURB)	Stepwise	outliers excluded	0.341	<0.0001
log(TURB), site, log(TURB)*discharge	log(TP)	Stepwise	outliers excluded	0.865	<0.0001
site, season, discharge, discharge*season	log(TP)	Stepwise	outliers excluded	0.431	<0.0001

Upstream Land Use

To further understand the results of the model with respect to sampling locations, the mean values of each parameter at each sampling location were correlated to upstream land use for both the existing water quality data and the grab sampling data. A summary of results is presented in Table 36 below.

Table 36: Upstream Land Use Regressions

Significant Predictor (X):	Response (Y):	Adjusted R^2	
		Existing Water Quality Data	Grab Sampling Data
% Agriculture	TSS	0.036	0.051
% Urban	TSS	0.083	0.074
% Agriculture	TP	0.135	0.106
% Urban	TP	0.016	0.147

Bivariate Regressions for Turbidity as a Predictor of TSS

Table 37 compares the bivariate regressions between TSS and Turbidity for both the existing water quality data and the grab sampling data. These models show how well Turbidity can be used to predict TSS based on the analysis of the data.

Table 37: Bivariate Regressions Predicting TSS as a Function of Turbidity

a.) Existing Water Quality Data:

Site	Site Name	Observations (n)	R^2	Probability (ά)
15	Yellow Brook @ Elton-Adelphia Rd.	14	0.794	< 0.0001
16-M	Squankum Brook @ Easy St.	14	0.028	> 0.05
Site 23	Mingamahone Brook @ Belmar Blvd.	14	0.030	> 0.05
Site 24	Marshes Bog Brook @ Preventorium Rd.	14	0.191	> 0.05
Site 25	Long Brook @ Howell Rd.	13	0.165	> 0.05
Overall		**69**	**0.559**	**< 0.0001**

b.) Grab Sampling Data:

Site	Site Name	Observations (n)	R^2	Probability (ά)
1	Manasquan River @ Georgia Rd.	12	0.861	<0.0001
2	Manasquan River @ Pointe of Woods Dr & Bergerville Rd.	12	0.964	<0.0001
3	Yellow Brook @ Adelphia-Farmingdale Rd.	11*	0.779	0.0002
4	Manasquan River @ Preventorium Rd.	12	0.951	<0.0001
5	Marshes Bog Brook @ Yellow Brook Rd.	11*	0.733	0.0005
6	Mingamahone Brook @ Allaire Rd.	11*	0.831	<0.0001
7	Manasquan River @ Hospital Rd.	12	0.935	<0.0001
Overall		**81****	**0.933**	**<0.0001**

* one (1) outlier excluded from analysis

** three (3) outliers excluded from analysis

Table 38: Bivariate Regressions Predicting TP as a Function of Turbidity

a. Existing Water Quality Data:

Site	Site Name	Observations (n)	R^2	Probability (ά)
15	Yellow Brook @ Elton-Adelphia Rd.	6	0.00364	> 0.05
16-M	Squankum Brook @ Easy St.	5	0.00014	> 0.05
Site 23	Mingamahone Brook @ Belmar Blvd.	5	0.00004	> 0.05
Site 24	Marshes Bog Brook @ Preventorium Rd.	5	0.27616	> 0.05
Site 25	Long Brook @ Howell Rd.	5	0.75654	> 0.05
Overall		**26**	**0.06975**	> 0.05

b. Grab Sampling Data:

Site Number	Site Name	Observations (n)	R^2	Probability (ά)
1	Manasquan River @ Georgia Rd.	12	0.924	<0.0001
2	Manasquan River @ Pointe of Woods Dr & Bergerville Rd.	11*	0.900	<0.0001
3	Yellow Brook @ Adelphia-Farmingdale Rd.	12	0.877	<0.0001
4	Manasquan River @ Preventorium Rd.	12	0.951	<0.0001
5	Marshes Bog Brook @ Yellow Brook Rd.	11*	0.881	<0.0001
6	Mingamahone Brook @ Allaire Rd.	11*	0.931	<0.0001
7	Manasquan River @ Hospital Rd.	12	0.929	<0.0001
Overall		**81****	**0.913**	**<0.0001**

* one (1) outlier excluded from analysis

** three (3) outliers excluded from analysis

Daily TSS and TP Loads

Table 39 compares the daily TSS and TP loads from WinSLAMM model results and calculated from grab sampling data. The tables below show how closely WinSLAMM modeled the potential loads of TSS and TP carried into the surface waters of the Manasquan Watershed.

There are some inherent limitations in the calculation of daily loads from the grab sampling data in Table 39b. The daily load calculation in tons/day is wholly dependent on the average daily discharge. Discharge at the time of grab sampling was taken solely from the USGS gauge station at Squankum. This gauge station is located on the main stem of the Manasquan River upstream of Site 4. As discussed earlier in this report, applying discharge values from a singular gauge station to all sites including those located on upstream reaches and on tributary streams will result in overestimated values in those areas.

Table 39: Comparison of WinSLAMM Model and Grab Sampling Results

a. WinSLAMM Model Results

Sampling Site	Sampling Location	Upstream WinSLAMM Subwatershed	WinSLAMM Model Results			
			Annual TSS Load	Annual TP Load	Daily TSS Load	Daily TP Load
			(tons/yr)	(tons/yr)	(tons/day)	(tons/day)
1	**Manasquan River @ Georgia Rd.**	**1**	**1,602**	**0.99**	**4.39**	**0.0027**
2	**Manasquan River @ Pointe of Woods Dr. & Bergerville Rd.**	**20**	**1,887**	**1.49**	**5.17**	**0.0041**
3	Yellow Brook @ Adelphia Farmingdale Rd.	12	880	1.11	2.41	0.0030
4	**Manasquan River @ Preventorium Rd.**	**22**	**3,471**	**4.13**	**9.50**	**0.0113**
5	Marshes Bog Brook @ Yellow Brook Rd.	15	1,248	1.42	3.42	0.0039
6	Mingamahone Brook @ Allaire Rd.	18	3,622	3.85	9.92	0.0105
8	**Manasquan River @ Hospital Rd.**	**24**	**4,528**	**5.21**	**12.40**	**0.0143**

b. Grab Sampling Results

Sampling Site	Upstream WinSLAMM Subwatershed	Average Daily Discharge @ Squankum		Grab Sampling Results (Average of 12 samples)					
				Mean TSS Values	Mean TP Values	Mean TSS Values	Mean TP Values	Mean Daily TSS Loads	Mean Daily TP Values
		(cfs)*	(gal/day)**	(mg/L)	(mg/L)	(tons/gal)**	(tons/gal)**	(tons/day)	(tons/day)
1	**1**	**69.33**	**44,807,625**	**22.5**	**0.169**	**9.38E-08**	**7.04E-10**	**4.20**	**0.0316**
2	**20**	**69.33**	**44,807,625**	**33.2**	**0.204**	**1.38E-07**	**8.50E-10**	**6.20**	**0.0381**
3	12	69.33	44,807,625	19.2	0.084	8.00E-08	3.50E-10	3.58	0.0157
4	**22**	**69.33**	**44,807,625**	**44.4**	**0.316**	**1.85E-07**	**1.32E-09**	**8.29**	**0.0590**
5	15	69.33	44,807,625	16.5	0.101	6.88E-08	4.21E-10	3.08	0.0189
6	18	69.33	44,807,625	20.5	0.119	8.54E-08	4.96E-10	3.83	0.0222
8	**24**	**69.33**	**44,807,625**	**44.3**	**0.299**	**1.85E-07**	**1.25E-09**	**8.27**	**0.0558**

Note: Sampling sites in bold are located on the main stem of the Manasquan River.
*Average daily discharge at Squankum USGS gauge station during grab sampling period (4/12/06 - 10/28/06).
**Conversion Factors
453,592 mg = 1 pound
2000 pounds = 1 ton
3.78 Liters = 1 gallon
1 cfs = 646272 gpd

Trends and Relationships in Datasets

Data Analysis Results

Tables 32 through 34 compares the summary statistics of the existing water quality data and grab sampling data. Water quality analyses of existing data resulted in values of: 15.6 ± 15.8 NTU for turbidity, 9.29 ± 6.90 mg/L for TSS, and 0.203 ± 0.281 mg/L for TP. Data from grab sampling measured: 36.8 ± 38.6 NTU for turbidity, 28.7 ± 30.8 mg/L for

TSS, and 0.185 ± 0.187 mg/L for TP. Automated water quality monitoring resulted in turbidity values of 25.46 ± 44.8 NTU. Existing water quality data is highly variable for TP and TSS, ranging as much as a magnitude of difference from the minimum value to the maximum value. It should be noted that existing water quality data was obtained mostly during baseflow conditions, and therefore peak values that would occur during storm events are not captured in the existing dataset. The existing water quality data was also obtained from multiple sources with different operating procedures and field personnel. This may explain some of the variability with existing dataset. Comparing summary statistics for turbidity data, results from the automated water quality monitoring phase of the project yielded the highest average values and largest range in values (2.0 – 579.4 NTU). Existing water quality data had the lowest average values (15.6 ± 15.8 NTU) and lowest range of values (2.90 – 75 NTU). Of the three datasets, the automated water quality monitoring allows for the capture of the greatest range of precipitation and runoff events. Grab sampling data allowed us to evaluate more storm events than the existing water quality data, but it is the automated water quality that gives the best overall picture of turbidity at varying conditions. Examining summary statistics for TSS, it is the results from grab sampling data that has higher average values (28.7 ± 30.8 mg/L) and a larger range (0.5 – 173 mg/L) as compared to the existing water quality data (9.29 ± 6.90 mg/L, range: (1 – 32 mg/L).

Table 35 presents the results of linear regression analysis performed on the existing water quality data and lab analysis results from the grab sampling phase of the project. The first model listed in both a.) and b.) of Table 34 evaluates turbidity as a predictor of TSS along with any significant effects from site location, seasonal variation and discharge. With the existing data, the resulting model showed turbidity, site, season and discharge as significant predictors of TSS ($\acute{\alpha} < 0.0001$, $R^2=0.590$). Analyzing the grab sampling data resulted in a linear regression model with turbidity and seasonal variation as the significant predictors of TSS ($\acute{\alpha} < 0.0001$, $R^2=0.787$). Discharge was examined for grab sampling data but it did not have a significant effect on the TSS/Turbidity relationship ($\acute{\alpha} = 0.4471$). The seasonal effect or the strength of Turbidity as a predictor may have masked the effect of discharge on this relationship. The model for grab sampling showed a much stronger fit with data indicating less variability within the dataset. This may be because all samples from grab sampling were handled by the same personnel and analyzed at the same laboratory.

The second model presented in Table 36 evaluates site location, seasonal variation and discharge effects on values of TSS. The model analyzing existing data had site, season, and discharge as significant predictors of TSS ($\acute{\alpha} < 0.0001$, $R^2=0.395$). There was also a significant site/season interaction effect associated with this model as well. The same parameters were used to analyze the grab sampling data and the model that was generated had seasonal variation and discharge as the most significant predictors of TSS ($\acute{\alpha} < 0.0001$, $R^2=0.355$). Additionally, this model also showed a discharge and seasonal variation interaction effect. Comparing these two models, the most obvious difference is the lack of site location as a significant predictor and the site/season interaction effect being replaced by a discharge/season interaction effect. Since grab sampling data was focused more on evaluating storm events versus the baseflow sampling that most of the existing water quality data is based on, these models would seem to indicate that discharge and seasonal variation have a much more important influence on TSS values during storm events as opposed to baseflow conditions. On the other hand, site location would appear to be more influential on TSS values during

baseflow conditions. Models for both datasets indicated a weak fit and the correlations could only explain 36-50% of the data based on the R^2 values.

The models on the third row of Table 35 evaluated site location, seasonal variation and discharge effect on turbidity values. The model analyzing existing data had site, season, and discharge as significant predictors of TSS (ά < 0.0001, R^2=0.444). There was also a significant site/season interaction effect associated with this model as well. The same parameters were used to analyze the grab sampling data and the model that was generated had seasonal variation and discharge as the most significant predictors of TSS (ά < 0.0001, R^2=0.341). The model based on the existing water quality data indicated site location, seasonal variation and discharge as significant predictors of turbidity values. The model based on the grab sampling data showed only season and discharge as significant predictors. As discussed in the previous paragraph, season and discharge appear to play more of a significant role on the grab sampling data which was focused on storm samples. Like the results of the second model, site location appears to be influential only on the existing water quality data.

The models shown on the fourth rows of Table 35 cannot be compared as they evaluate different parameters, since fecal coliform was not analyzed during the grab sampling phase of this project.

The models on the fifth row of Table 35 analyzed the effects of site, season and discharge on TP values. The model analyzing existing data had site, season, and discharge as significant predictors of TSS (ά < 0.0001, R^2=0.349). There was also a significant site/season interaction effect associated with this model as well. The same parameters were used to analyze the grab sampling data and the model that was generated had seasonal variation and discharge as the most significant predictors of TSS (ά < 0.0001, R^2=0.431). The model based on the existing water quality data indicated site location, and discharge as significant predictors of TP values. The model based on the grab sampling data showed site location, season and discharge as significant predictors. Additionally a discharge and season interaction effect also had a significant influence on TP values. Comparing these models, it is noted that seasonal variation is not a significant factor in the existing dataset but is important with the grab sampling data. Unlike TSS and Turbidity, this would seem to indicate that seasonal variation has a greater influence on TP values obtained during storm samples than during baseflow conditions.

Discharge appears to be the single factor that has the greatest influence on all of these parameters. It is listed as a significant predictor in nearly all of the models. Seasonal variation which is a factor in the variations of discharge throughout the year also seems to have a very strong effect on these relationships, particularly so with the grab sampling data. Lastly, evaluating the correlations between Turbidity and TSS as well as Turbidity and TP, these relationships appear to be very strongly correlated and would seem to indicate that Turbidity would be an adequate surrogate for those parameters.

Upstream Land Use Effects

Table 36 summarizes correlations with upstream land use and indicates that the upstream land use does significantly affect TP, and TSS values in both the existing water quality data and data from the grab sampling analysis. The analysis of grab sampling data shows that for both parameters, TP and TSS, the percentage of upstream

urban land use appears to have a greater influence on the model. With the existing water quality data, this holds true for TSS but not for TP where percent agriculture has a much stronger correlation with TP. However, as the results summarized in Table 35 indicate, the upstream land use alone does not explain the variability within the data set and results in poor model fits for both TP ($0.106 \leq R^2 \leq 0.147$) and TSS ($0.051 \leq R^2 \leq 0.074$) in the grab sampling data as well as poor model fits for TP ($0.016 \leq R^2 \leq 0.135$) and TSS ($0.036 \leq R^2 \leq 0.083$) with the existing water quality data.

Bivariate Regressions

The bivariate regressions that evaluate Turbidity as a predictor of TSS as summarized in Table 37 provide a very clear way to compare and contrast the datasets. The analysis of the existing water quality data was based on 69 observations overall and generated a significant correlation between Turbidity and TSS (R^2=0.559, ά<0.0001). Comparatively, the analysis of grab sampling data was based on 81 observations overall which generated an even stronger correlation between the two parameters (R^2=0.933, ά<0.0001). Table 37 also shows that the correlations are strong with the grab sampling data even when examined by site ($0.733 \leq R^2 \leq 0.951$) as opposed to the existing water quality data ($0.028 \leq R^2 \leq 0.794$) and do not vary nearly as much.

Bivariate regressions that evaluate Turbidity as a predictor of TP were also performed and are summarized in Table 38. The analysis of the existing water quality data was based on 26 observations overall and generated a very weak correlation between Turbidity and TP (R^2=0.06975, ά>0.05). Comparatively, the analysis of grab sampling data was based on 81 observations overall which generated an even stronger correlation between the two parameters (R^2=0.913, ά<0.0001). Table 38 also shows that the correlations are strong with the grab sampling data even when examined by site ($0.877 \leq R^2 \leq 0.951$) as opposed to the existing water quality data ($0.00004 \leq R^2 \leq 0.757$) and do not vary nearly as much. Samples for the TP analyses in the existing water quality dataset were collected by several different agencies and lab analyses were performed by multiple laboratories which may account for the significant discrepancy and lack of correlation.

Relationships between Data Analysis, Remote Sensing, and Watershed Modeling

Based on data analysis of existing water quality data, grab sampling data and data from the automated water quality monitoring stations, several general trends can be noted. Data from locations of grab sampling and automated water quality monitoring stations on or near segments identified by remote sensing analysis and verified by visual assessments and by watershed modeling as impaired or potential sediment sources (monitoring stations 2, 4 and 7, grab sampling sites 2 and 4) has tended to yield the highest values of TSS, Turbidity and TP. Inversely, grab sampling sites and monitoring stations located in areas identified by remote sensing and watershed modeling as of good or excellent health or as unlikely sources of sediment (monitoring stations and grab sampling sites 1, 3, and 5) generally have the lowest values of TSS, Turbidity and TP. Areas of moderate impairment as identified by watershed modeling and remote sensing such as monitoring stations 6 and 8 also showed moderate values for TSS, Turbidity and TP in the data analysis.

Data analysis has also shows that seasonal variation and discharge are the two most significant influences on the values of TSS, TP and Turbidity. Site location appears to

have more significance with baseflow conditions, but seasonal variation and discharge are more significant for stormflow conditions. Bivariate regressions and linear regression models also showed strong and significant correlations between Turbidity and TSS as well as Turbidity and TP.

Table 39 provides a way to evaluate the results of the WinSLAMM model by comparing relative daily TP and TSS loads results from the model to a calculation based on the grab sampling data collected. Although it is imperfect, due to the limitations of using a singular gauge station for discharge data and applying it to all sites, comparing the two sets of results does show relatively how accurate the WinSLAMM model is in predicting the pollutant loads from the watersheds. In general the WinSLAMM model appears to be relatively accurate in estimating the TSS loads with values ranging from 2.41 to 12.40 tons/day of TSS as compared with 3.08 to 8.29 tons/day of TSS for results from grab sampling. However, when comparing TP loads, the WinSLAMM model underestimates the values by a magnitude of difference with WinSLAMM results ranging from 0.0027 to 0.0143 tons/day of TP versus 0.0157 to 0.0590 tons/day of TP based on grab sampling results. Both sets of results do tend to show similar trends as has been seen in the other analyses, indicating higher values further downstream in the watershed and lower values located in the tributaries. Sites on the main stem of the Manasquan River also tend to have higher values in both sets of results. Results for the site at the Mingamahone Creek also have higher values than any of the other tributary sites.

Section 9 – Conclusions and Recommendations

Conclusions and Recommendations

Technical Memorandums have been provided for the designated tasks within this nonpoint source project. The Technical Memorandums were reviewed and analyzed by F. X. Browne, Inc. (FXB) for data accuracy, consistency with the project scope and condensed into this final Technical Report. The tasks reviewed were watershed modeling, remote sensing data, visual assessment and water quality monitoring. By comparing and contrasting all previous tasks, a recognizable pattern was developed that detailed the most significant sources of sediment loading to the Manasquan River. Twenty locations as shown on Figure 22: Proposed Selected Mitigation Areas were identified that exhibited the most severe deposition of silt and had the highest likelihood of success in lowering the levels of Total Suspended Solids (TSS), Turbidity (Tu) and Total Phosphorous (TP). These locations were categorized and evaluated for potential mitigation projects.

In Subwatershed 2, stream reaches 70 and 71 have major degradation concerns. The banks are severely eroded, debris has accumulated within the stream channel restricting flow, there is a bank cut from an unknown source and undercutting is present. The soils in this area are eroding and the overall drainage area has been densely developed. Possible projects in this area would be focused primarily on bank stabilization. The stream channels are constricted from debris in many locations. Clearing debris within the channel is necessary and channels can be stabilized by boulder toe revetment, installation of biologs, fascine, fiber rolls or willow wattles, as appropriate. At locations where convergent flow is entering the main channel some boulder toe protection is needed or the existing bank stabilization methods should be altered to stop bank erosion.

In Subwatershed 5, stream reaches 101, 103 and 111 have major degradation concerns. Stream reaches 101 and 103 both have areas of moderate to severe bank erosion and undercutting. Due to high storm velocities and unstable soils within these reaches, the erodible materials are depositing within the channel and along streambanks. In reach 101, residential stormwater outfall pipes are extending out of the streambanks due to bank erosion, and the discharge is causing further damage to the banks. In reach 103, there is a pedestrian foot bridge that needs stabilization to ensure the stability of the structure. Just downstream of the pedestrian bridge, an exposed utility line and a culvert end wall extending into the channel should be addressed. Downstream at reach 111, sediment has deposited as a result of upstream bank erosion. As a result of flashy storm flow events, the channel has downcut and no longer is connected to a functioning floodplain. There is also a road crossing culvert that needs to be repaired. Possible projects in this location would be an education program to inform homeowners about stormwater runoff, the importance of riparian buffers, and the impacts to the streams. Properties that directly discharge over the bank into the streams should be disconnected and discharged into the stream properly. Banks can be stabilized in many areas by removing sediment buildup and using plantings to stabilize banks. In areas where there is more severe undercutting and bank erosion, the use of biologs, vegetated mats, rip rap or boulder toe revetment can minimize bank loss and sediment deposition. The stabilization measures should re-connect the channel to an active floodplain.

In Subwatershed 6, stream reaches 126, 127, 129, 130, 134 and 135 have degradation concerns. Reaches 126, 127, 129, 130, 134 and 135 are all similar with moderate bank

erosion and debris accumulation within the channels. These areas pose major problems downstream with reaches 165 and 169, in Subwatershed 7. These areas are highly urbanized and contain erodible soils. Projects in these locations are vital to minimize sediment loads downstream and to maximize the success of projects completed downstream. Riparian buffer and bank planting can help mitigate many areas where bank erosion has taken place. Clearing debris from stream channels will also help alleviate bed and bank erosion and channel migration. In areas with more extensive bank erosion, the use of biologs, vegetated mats, boulder toe revetments, etc. should be utilized to stabilize the banks.

In Subwatershed 7, stream reaches 165 and 169 have accumulated sediment which is restricting flow, low to high severity bank erosion and undercutting, channel downcutting and an unknown channel that needs to be defined and channelized. This area also suffers from urbanization and poor soils that are highly susceptible to erosion. Possible projects for this location include clearing sediment bars and debris from channels. Redefining channel routes by incorporating natural channel design and reestablishing the low channel. The low to moderate severity bank cuts and erosion should be stabilized with native plantings. In areas of higher severity, the use of boulder toe revetments and the reconnection of the floodplain are necessary.

In Subwatershed 20, stream reach 13 has been degraded due to the upstream conditions in Subwatersheds 2, 4 and 5. Stream reach 13 has moderate to severe bank erosion in several locations, debris jams and sediment deposits in the bed and along the banks. Due to the large quantity of water this section carries during storm events, the channel has responded by over-widening and downcutting. We recommend clearing debris throughout the stream channel and removing the large amounts of sediment deposits to help redefine the reach. Channel stabilization is necessary in areas of bank erosion by boulder toe protection, fascines/wattles, biologs, revegetated stream banks, etc. and should include reconnecting the channel to the floodplain. Instream flow velocity reducers and channel stabilization structures such as Cross-Vanes, W-Weirs and J-Hook Vanes should be included in the stabilization design.

In Subwatershed 21, stream reaches 15, 17, 18, 203 and 23 have major degradation concerns. Stream reach 15 has severe bank erosion along both banks, at some locations the bank erosion is approximately 18' high. There is an outlet pipe overhanging the bank in one location that lacks structure and scour protection. Due to debris jams and the associated decreases in velocity, Reach 17 has large sediment deposits within the channel and along the banks from upstream erosion. The channel lacks definition due to bank erosion, sediment deposition and debris blockages. Reach 18 also endures erosion, sediment buildup and undercutting of the banks. There is an outlet structure that was not completed at the time of survey whose silt fencing surrounding the outlet has restricted flow, increasing erosion and sediment runoff at this location. Reach 203 enters the main stem at reach 18 junctions, at the unfinished outlet structure mentioned above. It has a lot of large woody debris restricting flow and low to moderate bank erosion. Reach 23 shows visible signs of the upstream erodible material throughout its bed. There is some undercutting and erosion of banks in this reach as well. The outlet structure in Reach 18 should be completed and cleared of debris to function properly. Severe bank erosion is evident in several locations and should be stabilized by boulder toe protection, vegetation of channel banks and reconnection of the floodplain. Sediment should be removed as appropriate to define the stream channel.

In Subwatershed 22, stream reaches 25, 30 and 31 have major degradation concerns. At reach 25, sediment deposition is clearly visible throughout the stream bed and banks. The banks are washing out at the base of the bridge on West Farm Road. A stormwater outlet structure enters here, but is blocked by sediment. At reach 30, sediment has accumulated at the road bridge within the channel and along the banks. An outlet pipe has protruded from the eroded bank. There is severe bank erosion in several locations and uncontrolled channels enter the reach at a few locations. In Subwatershed 23, reach 31 has lost channel definition and the banks have been undercut and severely eroded. Projects in this area should include removal of sediment to better define the channel. There are several locations where buildup has occurred along banks and point bars have been created within the stream bed. Streambank stabilization should also be completed to eliminate the erosion and undercutting potential of the banks. Stabilization within these areas can be done by using boulder toe revetments, biologs, vegetation of banks, etc. based on the severity of the problem.

In Subwatershed 18, stream reach 349 has been influenced from the upstream conditions of subwatersheds 17 & 18. Undercutting, bank erosion, sediment deposits and debris are evident throughout the channel. A road was washed out during a storm in 2005, due to lack of control within the channel. Projects for this reach are to revitalize this channel by clearing debris and stabilizing the banks.

In Subwatershed 24, stream reaches 382 and 40 have degradation concerns. In reach 382, severe sediment deposits have washed out from neighboring construction sites. The channel is blocked by debris jams which are restricting flow. Due to erodible soils and uncontrolled stormwater runoff flows, bank erosion, undercutting, and channel migration have also taken place throughout the reach. Reach 40 is the last reach within the watershed before the pump station. There is a large amount of sediment that has accumulated within this reach, as well as signs of undercutting and bank erosion. There are a few projects for reach 382 that will help eliminate sediment transportation. The channel should be cleared of large debris and sediment along banks and within the stream bed and the outlet structures should be stabilized to eliminate bank erosion. Proper maintenance of construction sites will avoid construction runoff from entering the streams and will prevent downstream sediment deposits. Providing proper silt fencing, grading, rock construction entrances are a few items that can help with eliminating runoff. Streambanks should be stabilized as described in the previous section. At the pump station within reach 40, sediment should be removed to avoid problems at the pump station and help guide flow through the channel properly.

Results of our study show how channel degradation within the watershed has occurred and the locations of where sediment loading is the greatest. The major causes of this loading include: debris blockages of stream channel restricting flow and degrading banks, lack of outlet structure control entering stream, and highly erodible soils that are easily transferable. The outcome of this degradation results in bank erosion, undercutting, lack of channel definition and sediment loading.

Figure 22: Proposed Mitigation Areas

The scope and extent of this study was limited to identifying likely sources of sediment loading to the NJWSA intake facility and formulating potential remediation strategies for those sources. Additional study will be needed to identify the source of the yellow coloration that appears in the surface waters of the watershed during the summer. Further investigation may also be needed to determine the effects of sediment resuspension on nutrient and trace metal loadings in the watershed. Further investigation should also be conducted to examine remediation strategies for subwatersheds with nutrient, solids and turbidity contributions but do not have a severe potential for channel destabilization. The effectiveness of strategies such as stormwater controls on individual lots, reducing the subsoil exposure during land disturbance and other preventative measures could reduce or eliminate the potential for nutrient and sediment loading from occurring in these subwatersheds.

References

Arnold, C. L., Jr., and C. J. Gibbons. 1996. *Impervious Surface Coverage The Emergence of a Key Environmental Indicator. Journal of the American Planning Association.* 62(2): 243-258.

Brant, T. & G. Kauffman. 2002. *The role of impervious cover as a watershed-based zoning tool to protect water quality in the Christina Basin of Delaware, Pennsylvania and Maryland.* Proceedings of the Water Environment Federation Conference, Watershed Management 2000. Vancouver, Canada

Center for Watershed Protection. 2003. *Impacts of Impervious Cover on Aquatic Systems.* Watershed Protection Research Monograph No. 1. Ellicott City, Maryland.

Cappiella, K. and K. Brown. 2001. *Land use and impervious cover in the Chesapeake Bay region.* Urban Lake Management. pp. 835-840.

Christensen, V. G., P. P. Rasmussen and A. C. Ziegler. 2002. *Comparison of Estimated Sediment Loads Using Continuous Turbidity measurements and Regression Analysis*. Turbidity and Other Surrogates Workshop, April 30-May 2, 2002, Reno, NV.

Kauffman, G.J., M. B. Corrozi, and K. J. Vonck. 2002. *Imperviousness: A performance measure of a Delaware water resource protection area ordinance.* Proceedings of the American Water Resources Association (AWRA) 2002 Summer Specialty Conference, Keystone, CO, July 1-3, 2002.

LaMotte Company. 2006. SMART Spectro Operator's Manual. LaMotte Company. Chestertown, Md.

Manasquan River Watershed Management Group (MWMG). 1999. *Manasquan River Watershed Initial Characterization and Assessment Report.*

Monmouth County. 1985. *Land Use in the Swimming and Manasquan River Reservoir Watersheds*. Monmouth County Planning Board. Freehold, NJ.

Monmouth County. 1999. *Municipal Acreage.* Data from the New Jersey Department of Environmental Protection 1986 GIS Data. Compiled by Monmouth County GIS Management Office. Freehold, NJ.

NJDEP. 1996. New Jersey 1996 *State Water Quality Inventory Report*. New Jersey Department of Environmental Protection, Office of Environmental Planning. Trenton, NJ.

NJDEP. 1997. *Draft Statewide Watershed Management Framework Document for the State of New Jersey*. New Jersey Department of Environmental Protection, Office of Environmental Planning. Trenton, NJ.

NJDEPE. 1993. *New Jersey 1992 State Water Quality Inventory Report.* New Jersey Department of Environmental Protection and Energy, Office of Land and Water Planning. Trenton, NJ

NJWSA. 2004. *Source Water Assessment Report for NJ Waster Supply Authority – Manasquan System*. New Jersey Water Supply Authority Watershed Protection Programs Unit. Somerville, NJ.

Robinson, R. B., C. D. Cox and K. Odom. 2005. *Identifying Outliers in Correlated Water Quality Data.* Journal of Environmental Engineering. 131 (4), pp. 651-657.

SAS Institute. JMP Statistics and Graphics Guide. Cary, North Carolina: SAS Institute Inc. 2002

Spiegel, M. R. Theory and Problems of Probability and Statistics. New York: McGraw-Hill, pp. 109-111, 1992.

Thomas, T. A. 1999. *Manasquan River Watershed Land Development Capacity* Analysis. T & M Associates. Middletown, NJ.

U.S. Department of Agriculture, Natural Resources Conservation Service, 2005. National Soil Survey Handbook, title 430-VI. [Online] Available: http://soils.usda.gov/technical/handbook/

Wischmeier, W.H. and Smith, D.D., 1978, *Predicting rainfall erosion losses: A guide to conservation planning,* Agriculture Handbook No. 537, U.S. Department of Agriculture, Washington D.C., 58 p.

YSI Incorporated. 2006. 6-Series Multiparameter Water Quality Sondes User Manual. YSI Incorporated. Yellow Springs, OH.

Appendices

Appendix A

Water Quality Statistical Models

Appendix B1

Grab Sampling Database and Data Summary

Appendix B2

JMP Grab Sampling Statistical Analyses

Appendix B3

JMP Grab Sampling Effects Tests Analyses

Appendix C

Stormwater Grab Sampling Guidance Document

Appendix D

Visual Assessments Photographs and Data Forms

Appendix E

Automated Water Quality Monitoring Data Summaries